

AperTO - Archivio Istituzionale Open Access dell'Università di Torino

The role of structural inheritance in continental break-up and exhumation of Alpine Tethyan mantle (Canavese Zone, Western Alps).

This is the author's manuscript

Original Citation:

Availability:

This version is available <http://hdl.handle.net/2318/1727793> since 2020-02-16T12:51:03Z

Published version:

DOI:10.1016/j.gsf.2018.11.007

Terms of use:

Open Access

Anyone can freely access the full text of works made available as "Open Access". Works made available under a Creative Commons license can be used according to the terms and conditions of said license. Use of all other works requires consent of the right holder (author or publisher) if not exempted from copyright protection by the applicable law.

(Article begins on next page)



UNIVERSITÀ DEGLI STUDI DI TORINO

This is an author version of the contribution published on:

Questa è la versione dell'autore dell'opera:

A. Festa; G. Balestro; A. Borghi; S. De Caroli; A. Succo, (2020)

*The role of structural inheritance in continental break-up and exhumation of Alpine Tethyan mantle (Canavese Zone, Western Alps). Geoscience Frontiers, **11**, 167-188*

The definitive version is available at:

La versione definitiva è disponibile alla URL:

<https://www.sciencedirect.com/science/article/pii/S1674987118302470>

Manuscript Number:

Title: The role of structural inheritance in continental break-up and exhumation of Alpine Tethyan mantle (Canavese Zone, Western Alps)

Article Type: SI: Ophiolites

Keywords: Alpine Tethys; Western Alps; Jurassic ophiolite; structural inheritance; continental break-up; mantle exhumation

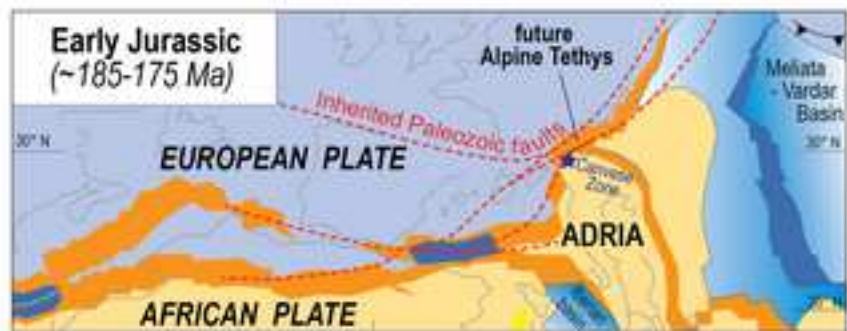
Corresponding Author: Professor Andrea Festa,

Corresponding Author's Institution: Universita di Torino

First Author: Andrea Festa

Order of Authors: Andrea Festa; Gianni Balestro; Alessandro Borghi; Sara De Caroli; Andrea Succo

Abstract: The Canavese Zone (CZ) in the Western Alps represents the remnant of the distal passive margin of the Adria plate, which was stretched and thinned during the Jurassic opening of the Alpine Tethys. Through detailed geological mapping, stratigraphic and structural analyses, we document that continental break-up of Pangea and tectonic dismemberment of the Adria distal margin, up to mantle rocks exhumation and oceanization, did not simply result from the syn-rift Jurassic extension but was strongly favored by older structural inheritances (the Proto-Canavese Shear Zone), which controlled earlier lithospheric weakness. Our findings allowed to redefine in detail (i) the tectono-stratigraphic setting of the Variscan metamorphic basement and the Late Carboniferous to Early Cretaceous CZ succession, (ii) the role played by inherited Late Carboniferous to Early Triassic structures and (iii) the significance of the CZ in the geodynamic evolution of the Alpine Tethys. The large amount of extensional displacement and crustal thinning occurred during different pulses of Late Carboniferous - Early Triassic strike-slip tectonics is well-consistent with the role played by long-lived regional-scale wrench faults (e.g., the East-Variscan Shear Zone), and suggest a re-discussion of models of mantle exhumation driven by low-angle detachment faults as unique efficient mechanism in stretching and thinning continental crust.



Graphical Abstract - Festa et al_ *Geoscience Frontiers* (5x13 cm)

1
1 2 **The role of structural inheritance in continental break-up and exhumation of**
2 3 **Alpine Tethyan mantle (Canavese Zone, Western Alps)**
3 3
4 4
5 5
6 6
7 6

8 7 ^{1*}Andrea Festa, ¹Gianni Balestro,
9 8 ¹Alessandro Borghi, ¹Sara De Caroli, and ²Andrea Succo
10 9

11 10
12 10
13 11
14 2
15 3
16 4
17 5 ¹Dipartimento di Scienze della Terra, Università di Torino, Torino, Italy

18 6 ²Dipartimento di Scienze Chimiche, della Vita e della Sostenibilità Ambientale, Università di Parma, Parma,
19 7 Italy
20 7
21 8
22 9
23 0
24 0
25 1
26 2
27 3
28 4
29 5
30 6
31 6
32 7
33 8
34 9
35 0
36 1
37 1
38 2
39 3
40 4
41 5

42 6 **Corresponding author:**

43 6 Dr Andrea Festa

44 7 Email: andrea.festa@unito.it
45 8
46 9
47 9
48 0
49 1
50 2

51 3 **Submitted to:**

52 2
53 4 Geoscience Frontiers

54 4 (Special Issue on “*Ophiolites: geodynamic and environmental implications*”)
55 5
56 6
57 7
58 8
59 9
60 0
61 1
62 2
63 3
64 4
65 5

48 **Abstract**

1
249
30 The Canavese Zone (CZ) in the Western Alps represents the remnant of the distal passive margin
4
51 of the Adria plate, which was stretched and thinned during the Jurassic opening of the Alpine
6
7
852 Tethys. Through detailed geological mapping, stratigraphic and structural analyses, we document
9
103 that continental break-up of Pangea and tectonic dismemberment of the Adria distal margin, up to
11
124 mantle rocks exhumation and oceanization, did not simply result from the syn-rift Jurassic
13
1455 extension but was strongly favored by older structural inheritances (the Proto-Canavese Shear
15
1656 Zone), which controlled earlier lithospheric weakness. Our findings allowed to redefine in detail (*i*)
17
18
1957 the tectono-stratigraphic setting of the Variscan metamorphic basement and the Late
20
2158 Carboniferous to Early Cretaceous CZ succession, (*ii*) the role played by inherited Late
22
2359 Carboniferous to Early Triassic structures and (*iii*) the significance of the CZ in the geodynamic
24
2560 evolution of the Alpine Tethys. The large amount of extensional displacement and crustal thinning
26
27
2861 occurred during different pulses of Late Carboniferous – Early Triassic strike-slip tectonics is well-
29
3062 consistent with the role played by long-lived regional-scale wrench faults (e.g., the East-Variscan
31
3263 Shear Zone), and suggest a re-discussion of models of mantle exhumation driven by low-angle
33
3464 detachment faults as unique efficient mechanism in stretching and thinning continental crust.
35
36
3765
38
3966
40

4167 **Key Words**

42
4368 Alpine Tethys, Western Alps, Jurassic ophiolite, structural inheritance, continental break-up, mantle
44
4569 exhumation
46
47
4870
49
5071
51
52
53
54
55
56
57
58
59
60
61
62
63
64
65

1. Introduction

During last decades a large interest has been dedicated in literature to processes and mechanisms of continental break up, mantle exhumation and sea-floor spreading related to the Jurassic rifting of the Alpine Tethys (i.e., the Ligurian – Piedmont Ocean). Comparison with present-day settings (e.g., Atlantic Ocean, see [Contrucci et al., 2004](#); [Moulin et al., 2005](#); Red Sea, see [Cochran and Karner, 2007](#); Norway passive margin, see [Osmundsen and Ebbing, 2008](#)) allowed to develop different modes of progressive stretching and lithospheric thinning, which may drive the sharp decrease in crustal thickness and strong decoupling between upper crust and continental mantle, up to continental breakup and mantle exhumation (e.g., [Brun and Beslier, 1996](#); [Péron-Pindvidic et al., 2007](#); [Ranero and Pérez-Guissinyé, 2010](#); [Clerc et al., 2018](#) and reference therein). These models were subsequently applied in different exhumed orogenic belts throughout the world as, for example, in the Alps ([Froitzheim and Eberli, 1990](#); [Manatschal et al., 2001](#); [Manatschal, 2004](#); [Mohn et al., 2010](#); [Beltrando et al., 2012](#); [Masini et al., 2012](#) and reference therein), Pyrenees (e.g., [Clerc et al., 2012](#); [Clerc and Lagabrielle, 2014](#)), and Betics (e.g., [Frasca et al., 2016](#)), independently by the structural and metamorphic complexities and polyphasic deformation of these regions. Here, less attention has been devoted to the potential role played by pre-Jurassic structural inheritance, which may have significantly controlled the location and kinematics of the Alpine Tethys rifting and mechanisms of mantle exhumation.

Structural inheritance may produce lateral variations in crustal thickness and thus in the rheology of both the continental crust and upper mantle lithosphere (e.g., [Armitage et al., 2010](#); [Aulin et al., 2013](#); [Spalla et al., 2014](#); [Phillips et al., 2016](#); [von Raumer et al., 2016](#); [Fazlikhani et al., 2017](#); [Marotta et al., 2018](#); [Will and Frimmel, 2018](#)). Multiple rifting events may have the same or different kinematics (e.g., [Talwani and Eldholm, 1972](#); [Armitage et al., 2010](#)) and, the rift trend may be inherited from a previous orthogonal rift stage (e.g., [Bonini et al., 1997](#); [Wolfeden et al., 2004](#)) or develop as the result of both specific far-field stresses and local weakness ([Bellahsen et al., 2006](#)) in the specific case of oblique rifting. Particularly, oblique extension may significantly facilitate the

100 rifting process and mantle exhumation, as oblique deformation requires less force in order to reach
101 the plastic yield limit than rift-perpendicular extension ([Brune et al., 2012](#); [Autin et al., 2013](#)).

102 However, although a general agreement exists among geoscientists on the important role of
103 structural inheritance in influencing and controlling the architecture and structural evolution of rifted
104 margins, other studies suggest that this role is most of the time local and unable to explain the non-
105 coincidence of early rifting stages and location of the final breakup (e.g., [Dunbar and Sawyer,](#)
106 [1989](#); [Bertotti et al., 1993](#); [Direen et al., 2008](#); [Lundin and Doré, 2011](#); [Manatschal et al., 2015](#) and
107 reference therein).

108
109 Discrimination on the role played by structural inheritances controlling the tectonic evolution and
110 structural deformation pattern of lithosphere and the onset of rifting stage is particular difficult to
111 decipher in orogenic belts. In fact, during their polyphasic tectonic and/or tectono-metamorphic
112 evolution, structural inheritances may be commonly (i) repeated reactivated (e.g., [Spalla et al.,](#)
113 [2014](#); [Ballèvre et al., 2018](#); [Balestro et al., 2018](#)), and/or (ii) masked by thick sedimentary and/or
114 magmatic sequences that also prevent detailed observation on the pre-rift crustal architecture
115 ([Ballèvre et al., 2018](#)).

116
117 In this paper, we document through multiscale, field- and laboratory- based structural studies (from
118 geological map scale to mesoscale and scanning electron microscope – SEM – scale), and re-
119 definition of the stratigraphic succession, the internal architecture, tectono-stratigraphic setting and
120 geological evolution of the Canavese Zone (CZ hereafter) in the Internal Western Alps ([Figs. 1A](#)
121 [and 1B](#)), which represents the remnant of the Jurassic syn-rift stretching, thinning and
122 dismemberment of the distal passive margin of Adria, occurred during the opening of the Alpine
123 Tethys (e.g., [Elter et al., 1966](#); [Bertotti et al., 1993](#); [Ferrando et al., 2004](#) and reference therein).

124 Particularly, we document that the Jurassic continental break-up and tectonic dismemberment of
125 the distal margin of Adria, up to mantle rocks exhumation, did not simply result from the syn-rift
126 Jurassic extension but was strongly favored by older structural inheritances (Variscan to Early
127 Triassic), which controlled earlier lithospheric weakness. Importantly, our findings are strongly

128 constrained on a new geological map at 1:5.000 scale of the entire CZ, a sector in which official
 1
 129 geological maps were older than one century of years (see [Franchi et al., 1912](#)).

3
 130
 5

6
 131
 7

8
 132

2. Regional Geological Setting

10
 133

12

134

14

135

15

136

16

137

17

138

18

139

19

140

20

141

21

142

22

143

23

144

24

145

25

146

26

147

27

148

28

149

29

150

30

151

31

152

32

153

33

154

34

155

35

156

36

The Canavese Zone ([Argand, 1909](#)) is discontinuously exposed in the Internal Western Alps ([Figs. 1A and 1B](#)), where it consists of a narrow zone, few kilometers wide and about 40 km long, bounded by two regional-scale first-order faults, about NE-striking, known as the Internal and External Canavese Lines (see [Biino and Compagnoni, 1989](#)). The Internal Canavese Line corresponds to an older left-lateral mylonitic contact (Late Cretaceous, [Schmid et al., 1987](#); [Biino and Compagnoni, 1989](#)), developed during low-grade Alpine metamorphism (i.e., prehnite–pumpellyite facies conditions; [Biino and Compagnoni, 1989](#); [Borghi et al., 1996](#)), which separates the CZ from the Ivrea - Verbano Zone of the S- and SE-verging Southern Alpine Domain ([Fig. 1B](#)) (see [Dal Piaz et al., 2003](#); [Schmidt et al., 2004](#)). The External Canavese Line ([Biino and Compagnoni, 1989](#)), which developed in Oligocene – Early Miocene time (e.g., [Lanza, 1984](#); [Biino and Compagnoni, 1989](#); [Berger et al., 2012](#)) under brittle conditions, corresponds to the southwestern prolongation of the Insubric Line or Peri-Adriatic Line ([Schmidt et al., 1987](#)), separating to NW the CZ from the Austroalpine Sesia Zone ([Fig. 1B](#)) and related Tertiary volcano-sedimentary cover ([Berger et al., 2012](#)). The Ivrea – Verbano Zone corresponds to a section of Adriatic lower crust, which consists of upper amphibolite – to granulite facies metasediments (the Kinzigite Formation *Auct.*), with mafic and ultramafic bodies, which were intruded by Lower Permian gabbro and diorite (the Mafic Complex *Auct.*; see [Zingg et al., 1990](#); [Quick et al., 2003](#)). It is tectonically juxtaposed along the Cossato – Mergozzo – Brissago Line *Auct.*, to the Serie dei Laghi ([Boriani and Sacchi, 1974](#); [Mulch et al., 2002](#)), consisting of two composite Variscan basement units (Strona Ceneri monometamorphic Unit and Scisti dei Laghi polymetamorphic Unit *Auct.*), which are separated by a horizon of amphibolites with lenses of ultramafic rocks called the Strona-Ceneri Border Zone ([Giobbi Mancini et al., 2003](#)). The two Variscan basement units,

156 consisting of metasediments and meta-intrusives, metamorphosed under amphibolite-facies
 1 conditions
 157 conditions ([Boriani et al., 1990](#)), were both intruded by Lower Permian granitoids, and covered by
 3 volcanic rocks and Permian to Cretaceous sediments ([Bertotti et al., 1993](#); [Boriani and Origoni](#)
 158 [Giobbi, 2004](#); [Quick et al., 2009](#)). The Sesia Zone, which is part of the NW-verging Alpine axial belt
 5
 159 (i.e., the Austroalpine Sesia-Dent Blanche nappes and the Penninic Domain), represents a
 7
 160 composite unit of Adriatic continental crust, which was metamorphosed under blueschist- to
 8
 161 eclogite facies conditions during the early building of the Alpine orogeny (e.g., [Spalla et al., 1991](#);
 10
 162 [Manzotti et al., 2014](#); [Giuntoli and Engi, 2016](#) and reference therein).
 12
 163
 14
 15
 16
 17
 18
 19

2065 The CZ, throughout its southern, central and northern sectors, is commonly described as
 21
 2266 consisting of a Variscan basement, Lower Permian igneous bodies and Permian to Lower
 23
 2477 Cretaceous pre-rift, syn-rift and post-rift sediments. The former has been distinguished into lower
 25
 2678 and upper crustal rocks (see [Ferrando et al., 2004](#)). Lower crustal rocks, occurring in the Southern
 27
 269 and Central sectors of the CZ (SCZ and CCZ hereafter, respectively), consist of migmatites
 30
 3170 intruded by anatectic leucogranite with enclaves of mafic granulite (e.g., [Baggio, 1965b](#); [Wozniak,](#)
 32
 3371 [1977](#); [Ferrando et al., 2004](#)) of Ivrea – Verbano Zone affinity. The upper crustal rocks consist of
 34
 3572 amphibolite-facies orthogneiss, micaschist and amphibolite, occurring in the CCZ (see [Wozniak,](#)
 36
 3773 [1977](#); [Borghi et al., 1996](#); [Ferrando et al., 2004](#)), and of greenschist-facies paragneiss, orthogneiss,
 38
 39
 4074 phyllite and metabasite, occurring in the northern sector of the CZ (NCZ hereafter; see [Biino and](#)
 41
 4275 [Compagnoni, 1989](#)). These upper crustal rocks, likely of Strona Ceneri Zone affinity ([Borghi et al.,](#)
 43
 4476 [1996](#); [Sacchi et al., 2007](#)), were intruded by Lower Permian granitoids at shallow crustal levels
 45
 4677 (see [Ferrando et al., 2004](#)). Lenticular-shaped slices of serpentized peridotite locally occur in the
 48
 4978 SCZ (Levone area, e.g., [Novarese, 1929](#); [Baggio, 1965a](#); [Elter et al., 1966](#); [Ahrendt, 1972](#);
 50
 5179 [Wozniak, 1977](#); [Barnes et al., 2014](#)).

5380 The Variscan basement is overlain by Lower Permian volcanics and volcanoclastics ([Fenoglio,](#)
 54
 5581 [1931](#); [Baggio, 1963a, 1965a, 1965b](#); [Sturani, 1964](#); [Elter et al., 1966](#); [Ahrendt, 1972](#); [Wozniak,](#)
 56
 57
 582 [1977](#); [Biino and Compagnoni, 1989](#); [Borghi et al., 1996](#); [Ferrando et al., 2004](#)), followed by pre-rift
 59
 6083 sediments of Permian to Triassic age (Verrucano *Auct.* and Middle Triassic dolostone; see [Elter et](#)
 61
 62
 63
 64
 65

184 al., 1966; Ferrando et al., 2004; Berra et al., 2009) and by Lower- to Middle Jurassic syn-rift
 185 sediments (“Macchia vecchia”, “Polymictic breccias”, “Levone breccias”; see Elter et al., 1966;
 186 Ferrando et al., 2004). The CZ sedimentary succession ends with a post-rift succession, Middle
 187 Jurassic to Early Cretaceous in age, consisting of Radiolarites (Middle – Late Jurassic), Maiolica
 188 micritic limestones (late Tithonian – Berriasian, see Baggio, 1963b), and Palombini shale (Early
 189 Cretaceous, see Baggio, 1965a; Elter et al., 1966). The entire Canavese succession is overprinted
 190 by Alpine metamorphism, which is limited to the anchizone and dated to 60-71,8 Ma (Zingg et al.,
 191 1976).

192
 193 Although primary relationships between the different terms of the Variscan basement and related
 194 sedimentary-volcanic cover succession are strongly complicated by Alpine deformation and
 195 faulting (e.g., Ahrendt, 1972; Wozniak, 1977; Biino and Comapagnoni, 1989; Borghi et al., 1996;
 196 Ferrando et al., 2004), low-angle detachment faults of Jurassic age were postulated to explain the
 197 juxtaposition of lower and upper crustal rocks and the mantle exhumation in the CCZ (Ferrando et
 198 al., 2014) and SCZ (Barnes et al., 2014), respectively. This deformation would have accompanied
 199 the evolution of the Ocean-Continental Transition zone (OCT) between the “hyperextended”
 200 passive margin of Adria and the Ligurian – Piedmont Ocean (Alpine Tethys). However, contrasting
 201 interpretations on the stratigraphic (e.g., Barnes et al., 2014 and reference therein) or tectonic
 202 (e.g., Novarese, 1929; Baggio, 1965a; Elter et al., 1966; Sturani, 1973) nature of the contact
 203 between Middle - Upper Jurassic (post-rift) radiolarian cherts and serpentinitized peridotites in the
 204 SCZ (Levone area) were differently proposed to support mechanisms of mantle exhumation
 205 through Jurassic (syn-rift) low-angle detachment faults or Alpine to neo-Alpine related tectonic
 206 slicing (see, e.g., Elter et al., 1966 for a complete discussion).

3. The Canavese Zone stratigraphy revisited

211 Detailed geological mapping and stratigraphic and structural analysis, allowed to revisit the
 1
 212 tectonically disrupted succession of the CZ (Fig. 2A), which consists of small slivers of
 3
 213 serpentized peridotites, a Variscan metamorphic basement, bodies of post-Variscan intrusives
 5
 214 and an Upper Carboniferous to Lower Cretaceous cover succession.

215 216 **3.1. Mantle rocks**

217 Slices of upper mantle rocks, limited to the SCZ (Fig. 2A), consist of massive serpentinite, passing
 14
 218 to sheared ones close to fault contacts (Fig. 3A). The serpentinite is composed by Cr-serpentine
 16
 219 and fine-grained magnetite, and by overprinted Cr-andradite and tremolite. The pre-
 18
 220 serpentization mineral assemblage is preserved as relics of clinopyroxene porphyroclasts, and as
 21
 221 mesh textures. The massive serpentinite is crosscut by pyroxenite dykes, centimeters to
 23
 222 decimeters in thickness, which mainly consist of clinopyroxene partly overprinted by epidote and
 25
 223 Mg-chlorite.

224 Major and trace element geochemistry is consistent with small to moderate mantle depletion of
 30
 225 sub-continental mantle rocks, while oxygen isotope data ($\delta^{18}\text{O}$ values: from +5.2 to +6.8), support
 32
 226 low-temperature serpentization (150° - 200°C) by sea-water at or near the seafloor (Barnes et al.,
 34
 227 2014).

228 229 **3.2. The Variscan metamorphic basement**

230 The characteristics of the Variscan basement can be defined in detail in the CCZ (Bric Figlia area;
 43
 231 Figs. 2A), wherein a poorly disrupted lithostratigraphic succession is exposed. It consists of two
 45
 232 tectonically superposed units (Lower and Upper units), which show different lithostratigraphic
 48
 233 successions and are separated by a discontinuous horizon of amphibolite (Figs. 4A, 4B and 4C).

50
 234 The two units were both metamorphosed under amphibolite-facies conditions during Variscan
 52
 235 orogeny.

53
 236
 57
 237 The Lower Metamorphic Unit (LMU hereafter) consists of medium- to coarse-grained orthogneiss,
 59
 238 tens to several hundreds of meters thick, deriving from pre-Variscan granitoid as shown by the

61
 62
 63
 64
 65

239 homogeneous structure with cm-sized porphyroclasts of K-feldspar and by the occurrence of layers
 1 of aplitic composition, centimeters in thickness. The orthogneiss (Fig. 3C) consists of altered
 240 plagioclase of oligoclase composition, quartz in plurimillimetric grains, K-feldspar in altered
 3
 241 idiomorphic crystals and annitic-rich red biotite. Minor white mica, Fe-Mg chlorite and Fe-epidote
 4
 242 also occur, together with rutile, apatite and association of zircon, monazite and allanite, as
 5
 243 accessory minerals. The Variscan foliation is pervasive and mainly defined by the preferred
 6
 244 orientation of biotite and of quartz-plagioclase aggregates. The Variscan mineral assemblage is
 7
 245 partly overprinted by pluri-centimeters granoblastic domains, consisting of (i) K-feldspar with
 8
 246 myrmekite intergrowth, (ii) polygonal quartz and (iii) idiomorphic oligoclase-andesine plagioclase
 9
 247 with antiperthite intergrowth of K-feldspar, and by non-oriented idiomorphic to allotriomorphic
 10
 248 crystals of biotite, garnet and white mica. Fibrous sillimanite and idiomorphic pseudomorph of white
 11
 249 mica after cordierite, also occur. These post-Variscan MT-HT minerals and fabrics highlight that the
 12
 250 orthogneiss was partly transformed into migmatitic gneiss (Fig. 3B). The latter is also characterized
 13
 251 by occurrences of garnet-rich restite and is associated with coarse-grained white mica-bearing
 14
 252 leucogranite of anatectic origin (see also Ferrando et al., 2004). The migmatitic gneiss and
 15
 253 leucogranite are spatially associated with intrusions of post-Variscan gabbro and diorite (Fig. 3B;
 16
 254 see below).

255
 256 The orthogneiss partly transformed into migmatitic gneiss and with associated leucogranite, also
 257 occur in the SCZ (Levone area; Fig. 2A), wherein they are tectonically juxtaposed to the above
 258 described mantle rocks through an Alpine faults.

259
 260 The orthogneiss are embedded and/or passes upward to fine-grained micaschist and medium-
 261 grained paragneiss, which show a maximum thickness of about few hundreds of meters (Figs. 4A,
 262 4B and 4C). The micaschist mainly consists of quartz, white mica, biotite locally associated with
 263 minor graphite, zoned garnet in millimeters wide porphyroblasts, plagioclase and chlorite. Similarly,
 264 the paragneiss consists of quartz, biotite, garnet and plagioclase, with minor K-feldspar. Zircon,
 265 apatite, rutile and titanite occur as accessory minerals both in the micaschist and paragneiss. The
 266 Variscan foliation is pervasive and is mainly defined by oriented white mica and biotite. The

267 Variscan mineral assemblage is locally overprinted by idiomorphic to allotriomorphic biotite and
 1 garnet, which statically grown during the post-Variscan MT-HT heating event. Unlike the
 268 orthogneiss, the metasediments of the LMU were not transformed into migmatites.
 3
 269
 5

270
 8
 271 The LMU and the overlying Upper Metamorphic Unit (UMU hereafter) are separated by a
 10 discontinuous horizon, up to ten meters thick, of amphibolite (Figs. 3D, 4A and 4B). The latter
 1072 mainly consists of amphibole of tschermakitic-pargasitic composition, occurring both in oriented
 12 lepidoblasts and in large crystal relics, and of plagioclase of oligoclase composition, occurring both
 1273 in idiomorphic porphyroclasts and altered porphyroblasts. The Variscan mineral assemblage also
 14 consists of titanite, rutile, apatite, zircon and epidote. The magmatic origin of the amphibolite is
 1574 suggested by the large idiomorphic crystal relics of amphibole and it likely derives from pre-
 16 Variscan effusive rocks of basaltic composition.
 17
 18
 19
 20
 21
 22
 23
 24
 25
 26
 27
 28

280 The UMU of the Variscan basement consists of alternating medium-grained metasandstone and
 30 fine-grained metasilstone (Figs., 3E, 4A and 4B), up to tens of meters thick, which are
 3081 characterized by preserved sedimentary organization in fining-upward horizons. These
 32 metasediments are locally interbedded with leucogneiss and fine-grained gneiss. The
 332 metasandstone and metasilstone consist of oriented plagioclase blasts of oligoclase composition,
 34 irregular to lobate oriented quartz grains, red biotite, and minor white mica lamellae and garnet
 3533 periclasts. The leucogneiss consists of meters-thick horizons made up of quartz, K-feldspar
 36 porphyroclasts, rounded granoblast of plagioclase, white mica, with minor biotite and rare garnet.
 37
 38
 39
 40
 41
 42
 43
 44
 45
 46
 47
 48
 49
 50
 51
 52
 53
 54
 55
 56
 57
 58
 59
 60
 61
 62
 63
 64
 65

293 The basement exposed in the NCZ (Lessolo and Montalto areas) is stratigraphically quite similar to
 1
 294 the UMU, but it was metamorphosed under greenschist-facies metamorphic conditions during the
 3
 295 Variscan orogeny (see [Biino and Compagnoni, 1989](#), and [Borghi et al., 1996](#)).

3.3. *The post-Variscan intrusives*

10
 298
 12
 299 In the whole CZ ([Fig. 2A](#)), the Variscan metamorphic basement was intruded by plutonic rocks and
 14
 300 hypoabissal dykes, and capped by volcanic rocks. Plutonic rocks are represented by a magmatic
 15
 16
 17
 301 suite consisting of up to 10 m sized bodies of gabbro, up to hundreds of meters wide bodies of
 18
 19
 202 diorite and tonalite, and kilometers sized granite plutons. The gabbro intruded rocks of the LMU in
 21
 203 the SCZ (Courgnè area; see [Biino et al., 1986](#)) and in the CCZ (Vidracco area), and it mainly
 23
 24
 304 consists of plagioclase, clinopyroxene and amphibole. The diorite and associated quartz-bearing
 25
 26
 305 diorite, intruded rocks of the LMU in the CCZ ([Fig. 3B](#)) and rocks of the UMU in the NCZ, and are
 27
 28
 296 composed of plagioclase, biotite, amphibole and clinopyroxene, whereas the tonalite occurs in the
 30
 307 CCZ and consists of plagioclase, quartz, K-feldspar and biotite. The whitish to pinkish granite
 32
 308 intruded rocks of the LMU and UMU, and consists of K-feldspar, quartz, plagioclase and biotite,
 34
 309 and locally shows diorite enclaves. The granite also occurs as dykes within the diorite ([Fig. 3F](#)).
 36
 37
 308 Plutonic rocks also consists of coarse-grained white mica-bearing leucogranite. The latter occurs
 38
 39
 401 as centimeters sized pods, decimeters wide dykes and tens of meters sized irregular masses,
 41
 402 which intruded the migmatitized orthogneiss as well as already cooled diorite. The leucogranite
 43
 44
 403 resulted from partial melting of the orthogneiss and its composition is similar to that of the quartz-
 45
 46
 404 feldspathic granoblastic domains overprinting the Variscan mineral assemblage in the orthogneiss.
 47
 48
 405 The hypoabissal dykes, up to decimeters wide, are widespread in the CCZ wherein intruded the
 50
 406 granite and the whole Variscan metamorphic basement ([Fig. 2A](#)), highlighting that both the LMU
 52
 407 and UMU, at time of dykes intrusion, were already exhumed at shallow crustal levels. They
 53
 54
 408 correspond to fine grained lamprophyre, dolerite and porphyry, mainly made up of plagioclase,
 55
 56
 409 biotite and amphibole, and to granophyre consisting of plagioclase, K-feldspar, quartz and biotite.

3.4. The Upper Carboniferous – Middle Triassic pre-extensional succession

Above a stratigraphic unconformity, which corresponds to the “Hercinian unconformity” *Auct.*, this succession shows significant lateral and vertical variations in both facies and thickness (Figs. 2A, 4A, 4B and 4C). The lower term corresponds to discontinuous continental fluvial deposits, up to few tens of meters in thickness, and consisting of clast- to matrix-supported conglomerates and coarse-grained sandstones (Fig. 3G). Clasts, rounded to irregular and up to decimeters in size, consist of metasandstone, micascist, gneiss and fragments of quartz veins. These clasts likely sourced from the UMU, which is the Unit unconformably covered by this fluvial deposit. The matrix, which lacks of any volcanic material, ranges from siltite to fine- to coarse-grained arenite and shows a very scarce maturity with angular shaped lithics of the same composition of clasts. This lithostratigraphic unit, occurring in the CCZ (Serra Alta; Figs. 2A and 3G) and never documented before, corresponds to the Upper Carboniferous – Lower Permian Basal Conglomerate *Auct.* of the Lombardian Basin (see, e.g., Cadel et al., 1996; Ronchi and Santi, 2003; Cassinis et al., 2012; Berra et al., 2016). Together with both the LMU and UMU of the Variscan basement, it is unconformably overlain by volcanic rocks and volcanoclastic deposits (Figs. 2A and 3H) comparable with part of the Lower Member of the Collio Formation *Auct.* (see, e.g., Cadel et al., 1996; Cassinis et al., 2012) of the Southern Alps, Early Permian in age. Volcanic rocks consist of microporphyric reddish and greenish fine-grained rhyolite and minor blackish pheno-andesite with local occurrence of clast-supported rhyolitic ignimbrites in decimeters thick bodies. The Collio Formation is characterized by significant and abrupt thickness variations (Fig. 2A), ranging from hundreds to tens, and up to zero meters across sectors tectonically juxtaposed along high-angle ENE- to NE-striking faults. Volcanoclastics rocks are commonly associated with the thicker portion of this succession (Fig. 2A), where they show wedge-like geometry that gradually pinches out laterally. They consist of angular clasts of both metamorphic and volcanic rocks, and fragments of glass, feldspar and biotite phenocrysts, embedded in a reddish to purple fine- to medium grained aphanitic matrix of the same composition with flame structures. Upwards, this succession shows a riodacitic composition, and is characterized by lenticular horizons, decimeters in thickness, with clasts and lithics of gneiss, metasandstone and volcanic rocks.

349 In the CCZ, lacustrine deposits, which consist of dark grayish thinly laminated siltite and claystone
 1
 350 beds, close upwards the volcanic member of the Collio Formation, resting unconformably onto both
 3
 351 the volcanic rocks and the Variscan metamorphic basement. Through an angular unconformity, the
 5
 352 Collio Formation is discontinuously overlain by reddish fluvial deposits of the Upper Permian
 7
 353 Verrucano (Figs. 2A and 3H), which consist of conglomerates and coarse-grained pebbly
 8
 354 sandstones with local siltstone layers (Fig. 3I). Pebble conglomerates are made of up to
 10
 355 centimeters in size clasts of granitoids, hypobasaltic dykes, volcanic and volcanoclastic rocks, and
 14
 356 metamorphic rocks sourced from both the LMU and UMU and the interposed mafic rocks (i.e.,
 16
 357 amphibolite, metasandstone, micaschist and orthogneiss). Single clasts of conglomerate, likely
 18
 358 sourced from the Upper Carboniferous – Lower Permian Basal Conglomerate *Auct.*, also occur.
 21
 359 Remarkably, some clasts of metasediments and of orthogneiss show occurrences of garnet
 23
 360 statically overprinting the Variscan mineral assemblages and of myrmekite intergrowth. This would
 24
 361 indicate a pre-Late Permian age of the post-Variscan MT-HT heating event.
 26
 362 As for the Collio Formation, the Verrucano shows significant thickness variations (from zero meters
 30
 363 to about 100 m) in sectors juxtaposed along ENE- to NE-striking faults (Figs. 4). Where the Collio
 32
 364 Formation is lacking, it directly overlies the Variscan metamorphic basement units and/or the Basal
 34
 365 Conglomerate.
 36
 37
 366
 39
 367 The Triassic deposits show the most complete succession in the CCZ. They start with non-
 41
 368 mappable greenish coarse-grained quartz-arenite, similar to the Lower Triassic Servino Formation
 42
 369 *Auct.* of the Lombardian Basin, passing upward to alternating black graphite-bearing clay-schist
 44
 370 and gray metasandstone layers, up to few meters thick. These sediments are followed by massive
 46
 371 dolomitic limestone and dolostone (Fig. 5A, San Salvatore Dolostone, see Elter et al., 1966;
 50
 372 Ferrando et al., 2004) of Middle Triassic age (Ladinic, see Berra et al., 2009) that, in the NCZ and
 52
 373 SCZ, are directly overlain onto the volcanic member of the Collio Formation and rocks of the LMU,
 54
 374 respectively, through a depositional hiatus (see also Berra et al., 2009) corresponding to Early
 55
 375 Triassic. The Triassic succession shows a maximum thickness of few tens of meters.
 57
 59
 376
 61
 62
 63
 64
 65

3.5. The Lower – Middle Jurassic syn-extensional succession

This Jurassic succession unconformably overlies all the above described lithostratigraphic sequence (Figs. 2A, 5A), marking a Late Triassic – Early Jurassic depositional hiatus (see, e.g., Berra et al., 2009). In the NCZ and CCZ, the top of platform dolostone is overlain by dolomitic breccias with a reddish matrix (Macchia Vecchia breccias type, see Baggio et al., 1965b; Bernoulli et al., 1990; Ferrando et al., 2004), which also fills Neptunian dykes and/or red and green arenaceous limestone, forming a Lower Sinemurian – Toarcian (?) condensed syn-extensional succession (Fig. 5A; see Sturani, 1963; Elter et al., 1966), related to the onset of the Jurassic rifting stage. This condensed succession, gradually opens far from platform deposits to form a complete syn-extensional succession, up to 80-100 m thick, here informally named Muriaglio Formation. It consists of four members with lateral and vertical facies variations throughout the CZ (Fig. 2A). The lower “Clastic Member” includes different types of matrix- to- clast-supported breccias whose components differ each other’s on the basis of the nature of the source area. In the CCZ, components consist of clast-to matrix-supported polymictic breccias (Polymictic breccias of Ferrando et al., 2004), with mainly sub-angular clasts, cm- to dm in size, embedded in a medium- to coarse-grained yellowish to reddish matrix, which unconformably overlain the Verrucano conglomerates and the Variscan metamorphic basement (Fig. 5B). Clasts are made of both units of the Variscan metamorphic basement (e.g., orthogneiss, amphibolite and metasandstone), volcanics and granitoids, and very rare Triassic dolostone (see also Ferrando et al., 2004). In the SCZ (Levone area; see Baggio, 1965b; Elter et al., 1966; Ferrando et al., 2004), the Clastic Member differs on the larger amount of Triassic dolomitic clasts and is unconformably overlain onto orthogneiss, migmatitic gneiss and leucogranite (Fig. 5C). In the NCZ, this member is reduced to few meters (Fig. 5D), while it reaches up to 40-50 m in thickness in the rest of the CZ. The age of the Clastic Member is tentatively attributed to Toarcian and/or late Early-Middle Jurassic by comparison with the Saluver Formation of the Australpine Err Nappe (see Ferrando et al., 2004). In the entire CZ, this member of the Muriaglio Formation gradually passes upward to the Arenaceous Member (roughly corresponding to the “Arenarie Rosse” of Baggio, 1965b; the “Grès volcanodétritiques” of Wozniak, 1977, and the “sandstone and black shale” of Ferrando et al.,

405 2004), which consists of alternating pelite and sandstone interbedded by dark-reddish argillitic
 1
 406 levels, millimeters in thickness, which increase in number and thickness upwards (Figs. 2A, 5E). It
 3
 407 passes upward and laterally to the Siltitic-arenaceous Member (Figs. 2A, 5F), which consists of
 5
 408 alternating pinkish marly limestones with crinoids fragments and greenish to reddish and yellowish
 7
 409 sandstone, in cm-thick horizons, interbedded by black pelitic to fine-grained sandstone levels with
 8
 10 sub-rounded clasts of yellowish quartz-rich arenite, centimeters in size. Only in the NCZ (Montalto
 110
 12 Dora sector), the upper part of the Muriaglio Formation is characterized by the Limestone Member
 13
 14 (corresponding to the Pistono Schist and Bio Schist *Auct.* of Biino and Compagnoni, 1989 and
 15
 16 reference therein), which consists of alternating limestone and sandstone in decimeters thick beds
 17
 18 (Figs. 2A, 5G). The age of the Muriaglio Formation, which shows gradual and abrupt changes of
 19
 20 thickness and facies in SW-NE and NW-SE direction (i.e., parallel and across ENE-to NE-striking
 21
 22 faults), respectively, is attributed to the upper part of Early Jurassic – Middle Jurassic (see Elter et
 23
 24 al., 1966 and reference therein).
 25
 26
 27
 28
 29
 30

3.6. The Upper Jurassic – Lower Cretaceous post-extensional succession

31 In the CCZ and SCZ, the Jurassic syn-extensional succession is unconformably overlain by post-
 32
 33 extensional deposits (Fig. 2A). They consist of reddish argillite, alternating with yellowish-greenish
 34
 35 pelite in decimeters thick horizons (Fig. 5H), passing upward and laterally to alternating reddish to
 36
 37 greenish radiolarian-bearing cherts and shale (i.e., Radiolarites *Auct.*; Fig. 5I), in meters thick
 38
 39 packages. Locally, the basal part of radiolarian cherts is interbedded by cm-thick layers of lithic
 40
 41 sandstone sourced from volcanic rocks and granitoids (see also Ferrando et al., 2004). This
 42
 43 composite unit, up to 40 m in thickness, shows strong similarities with the Selcifero Lombardo
 44
 45 Group of Southern Alps, and is attributed to Middle – Late Jurassic (see Elter et al., 1966;
 46
 47 Wozniak, 1977; Ferrando et al., 2004). Only locally (central part of the CCZ), the Selcifero
 48
 49 Lombardo is followed by Calpionella limestones (i.e., Maiolica of Baggio, 1963b) of Tithonian –
 50
 51 Berriasian age, which locally directly overlie the Variscan metamorphic basement and post-
 52
 53 Variscan intrusives (Fig. 2A). The Canavese succession is closed up by the Lower Cretaceous
 54
 55
 56
 57
 58
 59
 60
 61
 62
 63
 64
 65

432 Palombini shale (see [Elter et al., 1966](#)), which unconformably overlies the Variscan metamorphic
 1
 433 basement and the Jurassic succession ([Fig. 2A](#)).

3
 434
 5
 435
 7

436 **4. Structural setting and tectonic evolution**

10
 437

12
 438 The CZ corresponds to a narrow and complex polyphasic strike-slip deformation zone about NE-
 14
 439 striking ([Fig. 2A](#)), defined by the interlacing of high-angle and anastomized faults, ENE- to NE- and
 16
 440 E-striking, which isolate lenticular tectonic slices juxtaposing the different terms of the Paleozoic –
 18
 441 Mesozoic cover succession, the post-Variscan intrusives and the Variscan metamorphic basement.
 21
 442 To SW, in the SCZ, the main fault systems are gradually rotated to NNE-trending. The crosscut
 23
 443 relationships between the above described stratigraphic unconformities and mapped faults, allow
 25
 444 us to distinguish the characteristics of deformation through time as in the following.

26
 445
 28
 446

446 **4.1. Variscan deformation**

30
 447

34
 448 Both the units of the Variscan metamorphic basement and the interposed amphibolite are
 36
 449 overprinted by the same amphibolite-facies Variscan foliation, which is parallel to the lithological
 38
 450 contacts ([Figs. 4A, 4B and 4C](#)). In sectors (e.g., Bric Figlia in the CCZ, see [Fig. 4a](#)) escaped from
 39
 451 Alpine-related NE-striking reorientation (see below), it shows a roughly NW-striking orientation and
 41
 452 is almost NE dipping at medium angle ([Fig. 4A](#)). In the NCZ, the Variscan foliation shows similar
 43
 453 geometrical characteristics, whereas in the SCZ it is almost N-striking and E-dipping. This foliation
 45
 454 corresponds to the axial plane of isoclinal folds, which deformed a pre-existing early Variscan
 47
 455 foliation rarely preserved as a relic at fold hinges. The main foliation and the lithological contacts
 48
 456 within the basement are locally deformed by late Variscan open folds which roughly show E- and
 50
 457 W-plunging fold axis and N-dipping axial planes ([Fig. 4A](#)).

52
 458

54
 459 The Hercynian unconformity constrains this deformation of the Variscan metamorphic basement
 55
 460 before Late Carboniferous time ([Fig. 4](#)).

57
 461
 59
 462
 61
 463
 62
 464
 63
 465
 64
 65

4.2. Late Carboniferous to Early Permian faults

The different thickness and distribution of volcanic and volcanoclastic rocks of the Collio Formation in sectors juxtaposed along ENE- to NE-striking faults, well-agree with a tectonically controlled deposition during Early Permian time (Figs. 4A-C). In fact, the wedge-shaped volcanoclastic deposits, which pinch out laterally far from the faults, mainly occur in association with tectonically lowered sectors (Figs. 4B-E). Fault surfaces, which escaped from later deformation, and are sealed by the deposition of the lacustrine deposits of the Collio Formation and/or by the Verrucano, show both cartographic transtensional right-lateral and left-lateral movements (Figs. 4A-E). The uppermost temporal constrain to this tectonics is represented by the unconformable overlain of the lacustrine deposits of the upper part of the Collio Formation and of the fluvial Verrucano deposits (Late Permian) onto both the thin and thick volcanic sequence of the Collio Formation, and the LMU and UMU (Figs. 4A-E). The evidence that the volcanic member of the Collio Formation is directly overlain onto both the basement units (Figs. 4A-E), which are in turn juxtaposed along ENE- to NE-striking faults, also suggests that this fault activity likely started in Late Carboniferous as documented by the deposition of the Basal Conglomerate. Evidences of Early to Middle Permian fault activity is also documented by deformation-controlled emplacement of leucogranite which filled NE-striking fractures and associated faults (Fig. 3B).

4.3. Late Permian – Early Triassic faults

As for the Collio Formation, the different thickness of Verrucano deposits across ENE- to NE-striking faults, indirectly suggests their local reactivation in Late Permian – Early Triassic time (Figs. 4B-E). These faults depict divergent flower structures with “tulip” type geometry within the Verrucano and older lithostratigraphic units (Figs. 4B-C, 5N), in agreement with the continuation of transtensional movements as also suggested by paleomagnetic data (see Robustelli et al., 2018). The unconformable deposition of the Lower(?) and Middle Triassic succession onto either the Verrucano deposits, the Collio Formation, the post-Variscan intrusives and the Variscan metamorphic basement, constrains this faulting stage to pre-Middle Triassic (Fig. 2A).

4.4. Late Triassic – Early Jurassic faults (the Rifting stage)

The occurrence of an heterogeneous Lower Jurassic syn-extensional succession throughout the CZ, unconformably overlying the previously deformed Variscan metamorphic basement and related Upper Carboniferous – Middle Triassic cover succession (Figs. 2A, 4A-E), clearly documents the onset of the continental break-up related to the rifting of the Alpine Tethys (see, e.g., Elter et al., 1966; Bertotti et al., 1993; Ferrando et al., 2004; Berra et al., 2009). The about SW-NE gradual change of thickness and facies of the syn-extensional succession in sectors bounded by ENE- to NE-striking faults, which in turn also crosscut WNW- to W-striking faults (Fig. 4A), suggests that the Jurassic extension roughly occurred along a roughly E-W direction (present-day coordinates). The abrupt change of thickness and facies of the same syn-extensional succession across the long-lived ENE- to NE-striking faults, additionally suggest their reactivation, likely with transtensional movements. Although kinematic indicators directly correlated with this tectonic stage are dubitatively preserved because of subsequent reactivation (see below), map evidences tentatively suggest left-lateral movements, as also documented by Handy et al. (1999) to the NE. WNW- to W-striking faults are mainly SW-dipping at high-angle (Fig. 4A), and locally, as in the NCZ, the Middle Triassic platform dolostone preserves remnants of primary Jurassic tectonic-morphologic scarps toward which the syn-extensional Muriaglio Formation pinches-out, according to extensional displacements (i.e., fault striations and slickenlines mainly show normal-right movements). In this case, the syn-extensional breccias which drape the tectonic-morphological scarps mainly consist of dolostone clasts, sourced from the uplifted platform deposits (see Fig. 5C). On the contrary, where the syn-extensional clastic member of the Muriaglio Formation is directly overlain onto the Variscan basement and/or the Paleozoic succession, clasts mainly consist of these metamorphic rocks and very rarely of dolostone, as in the CCZ and SCZ (see Fig. 5B). In only one case in the CCZ (Bric Figlia area), the Clastic Member of the Muriaglio Formation rests unconformably onto an extensionally sheared Verrucano horizon, few meters thick and tens of meters long (Figs. 4A-B). The latter, which is characterized by the strong elongation of clasts according to a roughly ENE-oriented extensional stretching direction, is laterally bounded by NE-striking faults, close to which it is gradually reoriented. No other extensional low-angle shear

516 zones, comparable with the above described one, have been observed in the CZ. The maximum
 1
 517 vertical displacement of both these two main fault systems is of about few tens of meters (see [Figs.](#)
 3
 518 [4B-E](#)) as documented by the maximum thickness of syn-extensional deposits below the
 5
 519 uncoformable deposition of the post-extensional Selcifero Lombardo, Early – Middle Jurassic in
 7
 520 age. The latter, represents the uppermost temporal constrain to this deformation.

522 **4.5. Late Cretaceous – Early Miocene deformation (Alpine stage)**

523 The Alpine-related deformation is documented by different types of brittle to ductile structures,
 15
 524 which show different expression according to the rock rheology and distance from the Internal and
 17
 18
 19
 20
 21
 22
 23
 24
 25
 26
 27
 28
 29
 30
 31
 32
 33
 34
 35
 36
 37
 38
 39
 40
 41
 42
 43
 44
 45
 46
 47
 48
 49
 50
 51
 52
 53
 54
 55
 56
 57
 58
 59
 60
 61
 62
 63
 64
 65

External Canavese Lines, about NE-striking ([Fig. 2B](#)). Although out of the aim of this paper we
 shortly describe the characteristics of this deformation in that it is useful to discriminate the
 contribute played by older tectonic deformation. Close to these faults, the interlacing of
 anastomosing transpressional left-lateral faults, ENE- and NE-striking ([Fig. 2B](#)), defines a shear
 zone, hundreds of meters wide, along which several lenticular tectonic slices are juxtaposed,
 depicting flower structures at different scales in section. A pervasive cleavage oriented parallel to
 these faults and overprinted stratigraphic boundaries, according to simple shear deformational
 mechanisms. Tight to open folds with NE and SW-plunging axis also occur ([Fig. 4A](#)). In the NCZ,
 this deformation is close associated with mylonitic deformation, which juxtaposed the Limestone
 Member of the Muriaglio Formation with the gabbros of the Ivrea - Verbano Zone ([Fig. 5L](#); see,
[Biino and Compagnoni, 1989](#) for major details). Far from both the Internal and External Canavese
 Lines, the cleavage, which occurs as spaced surfaces ENE- to NE-striking, cuts at high angle the
 stratigraphic contacts according with pure shear deformation mechanisms. Kinematic indicators on
 ENE- to NE- and W- to WNW-striking faults, are consistent with a roughly NNE-oriented shortening
 direction ([Fig. 2B](#)), indicating transpressional left-lateral and oblique to reverse movements. Both
 these fault systems, displace all the stratigraphic succession up to the younger term, which
 correspond to the Palombini shale ([Figs. 2A, 4A](#)), constraining their age to post- Early Cretaceous,
 according to the eo-Alpine deformation.

543 The superposition of transtensional right-lateral movements on ENE- to NE-striking faults, which
 1 agree with a WNW-oriented regional shortening direction (Fig. 2B), document a further reactivation
 544 3 of previously existing faults. In the NCZ, these faults obliquely cut the mylonitic deformation (i.e.,
 545 5 of previously existing faults. In the NCZ, these faults obliquely cut the mylonitic deformation (i.e.,
 546 7 the Internal Canavese Line *sensu* Biino and Compagnoni, 1989) that juxtaposes the CZ and the
 547 8 Ivrea – Verbano Zone (Fig. 5L). This suggests that the present-day contact between these two
 10 zones corresponds to a younger brittle shear zone, likely reactivated during the tectonic
 548 12 exhumation of the Sesia Zone along the External Canavese Line (Fig. 5M). Although stratigraphic
 549 14 markers to temporal constraint this fault activity are lacking, it is well comparable with the
 550 16 Oligocene – Early Miocene tectonics which displaced Oligocene volcanics to the North of the
 551 18 studied sector (e.g., Berger et al., 2012; see also Lanza, 1984).
 552 21

553 23

554 25

555 27

556 28

557 30

558 32

559 34

560 36

561 38

562 40

563 42

564 44

565 46

566 48

567 50

568 52

569 54

570 56

571 58

572 60

573 62

574 64

575 66

576 68

577 70

578 72

579 74

580 76

581 78

582 80

583 82

584 84

585 86

586 88

587 90

588 92

589 94

590 96

591 98

592 100

593 102

594 104

595 106

596 108

597 110

598 112

599 114

600 116

601 118

602 120

603 122

604 124

605 126

606 128

607 130

608 132

609 134

610 136

611 138

612 140

613 142

614 144

615 146

616 148

617 150

618 152

619 154

620 156

621 158

622 160

623 162

624 164

625 166

626 168

627 170

628 172

629 174

630 176

631 178

632 180

633 182

634 184

635 186

636 188

637 190

638 192

639 194

640 196

641 198

642 200

643 202

644 204

645 206

646 208

647 210

648 212

649 214

650 216

651 218

652 220

653 222

654 224

655 226

656 228

657 230

658 232

659 234

660 236

661 238

662 240

663 242

664 244

665 246

666 248

667 250

668 252

669 254

670 256

671 258

672 260

673 262

674 264

675 266

676 268

677 270

678 272

679 274

680 276

681 278

682 280

683 282

684 284

685 286

686 288

687 290

688 292

689 294

690 296

691 298

692 300

693 302

694 304

695 306

696 308

697 310

698 312

699 314

700 316

701 318

702 320

703 322

704 324

705 326

706 328

707 330

708 332

709 334

710 336

711 338

712 340

713 342

714 344

715 346

716 348

717 350

718 352

719 354

720 356

721 358

722 360

723 362

724 364

725 366

726 368

727 370

728 372

729 374

730 376

731 378

732 380

733 382

734 384

735 386

736 388

737 390

738 392

739 394

740 396

741 398

742 400

743 402

744 404

745 406

746 408

747 410

748 412

749 414

750 416

751 418

752 420

753 422

754 424

755 426

756 428

757 430

758 432

759 434

760 436

761 438

762 440

763 442

764 444

765 446

766 448

767 450

768 452

769 454

770 456

771 458

772 460

773 462

774 464

775 466

776 468

777 470

778 472

779 474

780 476

781 478

782 480

783 482

784 484

785 486

786 488

787 490

788 492

789 494

790 496

791 498

792 500

793 502

794 504

795 506

796 508

797 510

798 512

799 514

800 516

801 518

802 520

803 522

804 524

805 526

806 528

807 530

808 532

809 534

810 536

811 538

812 540

813 542

814 544

815 546

816 548

817 550

818 552

819 554

820 556

821 558

822 560

823 562

824 564

825 566

826 568

827 570

828 572

829 574

830 576

831 578

832 580

833 582

834 584

835 586

836 588

837 590

838 592

839 594

840 596

841 598

842 600

843 602

844 604

845 606

846 608

847 610

848 612

849 614

850 616

851 618

852 620

853 622

854 624

855 626

856 628

857 630

858 632

859 634

860 636

861 638

862 640

863 642

864 644

865 646

866 648

867 650

868 652

869 654

870 656

871 658

872 660

873 662

874 664

875 666

876 668

877 670

878 672

879 674

880 676

881 678

882 680

883 682

884 684

885 686

886 688

887 690

888 692

889 694

890 696

891 698

892 700

893 702

894 704

895 706

896 708

897 710

898 712

899 714

900 716

553 23

554 25

555 27

556 28

557 30

558 32

559 34

560 36

561 38

562 40

563 42

564 44

565 46

566 48

567 50

568 52

569 54

570 56

571 58

572 60

573 62

574 64

575 66

576 68

577 70

578 72

579 74

580 76

581 78

582 80

583 82

584 84

585 86

586 88

587 90

588 92

589 94

590 96

591 98

592 100

593 102

594 104

595 106

596 108

597 110

598 112

599 114

600 116

601 118

602 120

603 122

604 124

605 126

606 128

607 130

608 132

609 134

610 136

611 138

612 140

613 142

614 144

615 146

616 148

617 150

618 152

619 154

620 156

621 158

622 160

623 162

624 164

625 166

626 168

627 170

628 172

629 174

630 176

631 178

632 180

633 182

634 184

635 186

636 188

637 190

638 192

639 194

640 196

641 198

642 200

643 202

644 204

645 206

646 208

647 210

648 212

649 214

650 216

651 218

652 220

653 222

654 224

655 226

656 228

657 230

658 232

659 234

660 236

661 238

662 240

663 242

664 244

665 246

666 248

667 250

668 252

669 254

670 256

671 258

672 260

673 262

674 264

675 266

676 268

677 270

678 272

679 274

680 276

681 278

682 280

683 282

684 284

685 286

686 288

687 290

688 292

689 294

690 296

691 298

692 300

693 302

694 304

695 306

696 308

697 310

698 312

699 314

700 316

701 318

702 320

703 322

704 324

705 326

706 328

707 330

708 332

709 334

710 336

711 338

712 340

713 342

714 344

715 346

716 348

717 350

718 352

719 354

720 356

721 358

722 360

723 362

724 364

725 366

726 368

727 370

728 372

729 374

730 376

731 378

732 380

733 382

734 384

735 386

736 388

737 390

738 392

739 394

740 396

741 398

742 400

743 402

744 404

745 406

746 408

747 410

748 412

749 414

750 416

751 418

752 420

753 422

754 424

755 426

756 428

757 430

758 432

759 434

760 436

761 438

762 440

763 442

764 444

765 446

766 448

767 450

768 452

769 454

770 456

771 458

772 460

773 462

774 464

775 466

776 468

777 470

778 472

779 474

780 476

781 478

782 480

783 482

784 484

785 486

786 488

787 490

788 492

789 494

790 496

791 498

792 500

793 502

794 504

795 506

796 508

797 510

798 512

799 514

800 516

801 518

802 520

803 522

804 524

805 526

806 528

807 530

808 532

809 534

810 536

811 538

812 540

813 542

814 544

815 546

816 548

817 550

818 552

819 554

820 556

821 558

822 560

823 562

824 564

825 566

826 568

827 570

828 572

829 574

830 576

831 578

832 580

833 582

834 584

835 586

836 588

837 590

838 592

839 594

840 596

841 598

842 600

843 602

844 604

845 606

846 608

847 610

848 612

849 614

850 616

851 618

852 620

853 622

854 624

855 626

856 628

857 630

858 632

859 634

860 636

861 638

862 640

863 642

864 644

865 646

866 648

867 650

868 652

869 654

870 656

871 658

872 660

873 662

874 664

875 666

876 668

877 670

878 672

879 674

880 676

881 678

882 680

883 682

884 684

885 686

886 688

887 690

888 692

889 694

890 696

891 698

892 700

893 702

894 704

895 706

896 708

897 710

898 712

899 714

900 716

571 documented before, is interposed (Figs. 6A-B). Importantly, far from the main faults, Middle
 1
 572 Triassic massive dolostone originally cropped out, likely in primary stratigraphic contact between
 3
 573 the Early Permian volcanics of the Collio Formation and the post-extensional Selcifero Lombardo
 5
 574 (see Novarese, 1929; Baggio, 1965a). Although they are now lacking because of intense quarry
 6
 575 activity, we have restored the primary position of dolostone in Fig. 6 according to literature data
 8
 576 (Novarese, 1929; Baggio, 1965a). A NNW-trending cleavage (i.e., parallel to the main fault) also
 10
 577 occurs and can be related with Alpine deformation. Cataclastic deformation related to this stage
 14
 578 also affects volcanic rocks along the main faults. Regional-scale N-S trending strike-slip faults has
 15
 579 been also detected SW of the SCZ, along the inner sector of the Alpine accretionary wedge (see
 17
 580 Balestro et al., 2009, and Perrone et al., 2010)
 18
 19
 20
 21
 22
 23
 24
 25

583 6. Discussion

584
 585 In this section we discuss in a regional tectonic framework the significance of our multidisciplinary
 32
 586 and multiscale data from the CZ to redefine: (i) the nature and characteristics of the Variscan
 34
 587 metamorphic basement, (ii) the role played by Late Carboniferous to Early Triassic structural
 35
 588 inheritance in the break-up of the passive continental margin of Adria and Alpine Tethyan mantle
 36
 589 exhumation, and (iii) the significance of the CZ in the geodynamic evolution of the Alpine Tethys.
 37
 38
 39
 40
 41
 42
 43

591 **6.1. Redefinition of the Variscan metamorphic basement and its nature**

592 Our data show that the Variscan basement of the CZ consists of two superposed units (i.e., the
 47
 593 LMU and UMU), which are characterized by different stratigraphy and are separated by a
 48
 50
 594 discontinuous horizon of mafic rocks. The tectonic coupling between these units is constrained to
 52
 595 Variscan time by the common amphibolite-facies Variscan metamorphic foliation overprinting the
 53
 596 two units in the CCZ.
 54
 55
 56

597 In the UMU, the occurrence of preserved sedimentary textures in both the metasandstone and
 57
 59
 598 metasilstone, suggests that these metasediments correspond to a monometamorphic complex
 60
 61
 62
 63
 64
 65

599 and derive from a sedimentary and volcanic succession likely of Silurian – Devonian age. On the
1
600 contrary, the pervasive deformation and the absence of preserved stratigraphic markers, would
3
601 suggest that the metasediments of the LMU (i.e., the micaschist) correspond to a polymetamorphic
5
602 complex. This would also be highlighted by the occurrence of bodies of orthogneiss within the
7
603 micaschist, suggesting that pre-Variscan granitoid, likely of Ordovician age, intruded an already
9
10
604 metamorphosed basement. The discontinuous occurrence of up to 10 m thick amphibolite, likely of
12
605 basaltic origin, interposed between the LMU and the UMU, is well-comparable with the internal
14
606 structure of the Southern Alpine metamorphic basement where it is inferred to mark a Variscan
16
607 tectonic contact (i.e., The Strona Ceneri Border Zone; [Giobbi-Origoni et al., 1982](#); [Boriani et al.,](#)
18
608 [1990](#)). Thus, our findings suggest an affinity between the LMU and UMU and the Scisti dei Laghi
21
609 polymetamorphic complex and Strona Ceneri monometamorphic complex of the Southern Alpine
23
610 Domain (Serie dei Laghi *Auct.*), respectively. Both the complexes were intruded by granitoid of
25
611 Ordovician age, and are tectonically separated by slices of mafic and ultramafic rocks (e.g., [Giobbi-](#)
27
612 [Origoni et al., 1982](#); [Boriani et al., 1990](#)). Similar interpretations were already proposed by [Borghi](#)
30
613 [et al. \(1996\)](#) and [Sacchi et al. \(2007\)](#) for the NCZ and CCZ.

31
32
33
34
615 Plutonic rocks correspond to a magmatic suite consisting of minor gabbro, diorite and tonalite, and
36
616 of widespread granite, which intruded rocks both of the LMU and UMU. The occurrence of
37
38
39
617 hypoabissal dykes within granitoid bodies highlights the existence, within the same magmatic
41
618 event, of a first intrusive stage followed by a mixed intrusive and volcanic one. These dykes also
43
619 occur in the LMU and UMU, proving that the whole Variscan basement was located at a shallow
45
620 crustal level at time of intrusion.

48
49
50
622 This overall magmatic activity can be referred to that one of the Sesia Magmatic System, which
52
623 affected the upper crust of the Serie dei Laghi (i.e., “Graniti dei Laghi” *Auct.*) and the lower crust of
54
55
624 the Ivrea - Verbano Zone (i.e., “Mafic Complex” *Auct.*) in Early Permian age ([Quick et al., 2009](#) and
57
58
59
625 reference therein; see also [Pin, 1986](#); [Mayer et al., 2000](#)), with different pulses of mafic to acidic
61
62
63
64
65
626 plutonic activity and volcanism within 10 Ma intervals (about 290 and 280 Ma), and with ascent and

627 emplacement of magmas facilitated by transextensional faulting (Rottura et al., 1998; Handy and Steit,
1
628 1999; Handy et al., 1999).

3
4
5
6
630 Partial melting of the orthogneiss of the LMU is highlighted by its partial transformation into
7
8
631 migmatite and by occurrence of pods, dykes and irregular masses of white mica-bearing
9
10
632 leucogranite, which also emplaced within already cooled gabbro and diorite, and filled coeval NE-
11
12
633 striking faults and fracture systems. The spatial association of the gabbro and diorite bodies with
13
14
634 this anatectic leucogranite, would highlight that they represent the heating source for the partial
15
16
635 melting process. The existence of a general heating event is also constrained by static growth of
17
18
636 MT-HT minerals (i.e., biotite, white mica and garnet) in the micaschist of LMU. Since single clasts
19
20
637 of the Verrucano deposits show evidences of this heating event, the latter could be regarded as of
21
22
23
638 pre-Upper Permian age. As a matter of fact, a biotite from migmatitic gneiss of the CCZ has been
24
25
639 dated as Middle Permian (264.0 ± 3.9 Ma; Beltrando et al., 2014). This post-Variscan heating can be
26
27
28
640 overall related to the so-called Permian HT metamorphic event (Schuster and Stuwe, 2008; Spalla
29
30
641 et al., 2014), well-documented in the Southern Alpine Domain. Although this event is mainly
31
32
642 recorded and documented in the Ivrea-Verbano lower crust, it also matched with “appinite” mafic to
33
34
643 intermediate intrusions, which emplaced along the Cossato-Mergozzo-Brissago Line (i.e., the
35
36
644 shear zone separating the Ivrea-Verbano zone from the Serie dei Laghi *Auct.*, Garde et al., 2015,
37
38
39
645 and reference therein) and locally induced partial melting (Mulch et al., 2002). The amphibole-
40
41
646 bearing gabbro and diorite in the CZ are very similar to the appinite and, remarkably, they are
42
43
647 spatially associated to the migmatitic gneiss in the study area.

44
45
648 As discussed in the following, the overall relationships between the architecture of the Variscan
46
47
649 basement, emplacement of the post-Variscan intrusives and heating event in the CZ, have to be
48
49
50
650 seen in the more general context of the strike-slip tectonics and crustal thinning which controlled
51
52
651 magmatic activity and affected the Adriatic crust during the Permian period along the “Proto-
53
54
652 Canavese Shear Zone” (see below).

55
56
57
653
58
59
60
61
62
63
64
65

6.2. Role of structural inheritance in the break-up of the passive continental margin of Adria and Jurassic mantle exhumation

After the Variscan orogeny, different pulses of a Late Carboniferous to Early Triassic strike-slip tectonics, which are documented for the first time in the CZ, are well-constrained through the crosscutting relationships between stratigraphic unconformities and mapped faults. In fact, the evidence that the Collio Formation is directly overlain onto both the LMU and UMU (Figs. 2A and 4), which are in turn juxtaposed along ENE- to NE-striking faults, suggests that this fault activity likely started since Late Carboniferous as also documented by the larger amount of displacement accommodated in the basement with respect to that observed within the Lower Permian succession (Fig. 4). In addition, above the Hercynian unconformity, the different thickness of the volcanic member of the Collio Formation, clearly documents deposition on structural highs and lows, bounded by ENE- to NE-striking (present day coordinates) transtensional faults (Figs. 4 and 7A), as well-documented in the Southern Alps during Early Permian – Early Triassic (see, e.g., Handy and Zingg, 1991; Cadel et al., 1996; Handy et al., 1999; Spalla et al., 2014; Marotta et al., 2018 and reference therein). This faulting activity continued with alternating intensity up to the unconformable overlain of the fluvial deposits in Verrucano facies (Late Permian), as well stated by the first partial sealing of the faults by lacustrine deposits of the upper part of the Collio Formation, and by the different thickness of Verrucano deposits (Figs. 4C and 4E). The occurrence in the Verrucano of clasts sourced from both the units of the Variscan metamorphic basement, volcanic rocks and intrusives, highlights that these different basement units were already exhumed in Late Permian. This is also supported by the direct overlain of Middle Triassic dolostone onto the different Paleozoic rocks and the Verrucano (Figs. 2A and 7A). Similar observations are also documented NE of the studied sector in the Southern Alps (see, e.g., Handy and Zingg, 1991; Handy et al., 1999 and reference therein). Here ENE-trending transtensional left-lateral faults (i.e., the Cossato – Mergozzo – Brissago Line) controlled both the deposition of the Collio Formation in narrow and elongated basins, and the exhumation of the lower crust in the Ivrea – Verbano Zone. Particularly, Handy et al. (1999) suggested, on the basis of petrological data, that different thermal pulses occurred after Carboniferous time, playing a significant role in affecting the pre-Alpine crust,

682 potentially related with (and also following) the asthenospheric upwelling driven by the Late
1
683 Triassic – Early Jurassic hyper-extension of the Adria margin (see also [Smye and Stockli, 2014](#)).
3
684
5
685 The above described articulated tectono-stratigraphic setting, above which the Triassic platform
6
686 succession deposited, thus represents the structural inheritance at the onset of the Early Jurassic
8
687 continental break-up of the passive margin of Adria ([Fig. 7A](#)). The gradual and abrupt change of
10
688 facies and thickness of syn-extensional sediments (i.e., Muriaglio Formation) parallel (i.e., SW-NE
12
689 direction) and across (i.e., NW-SE direction) of long-lived inherited faults, ENE- to NE-striking,
14
690 document their syn-depositional reactivation in Early Jurassic, likely as transtensional faults. The
16
691 evidence that they bound SW-dipping high-angle extensional faults and, only in one case (in the
18
692 Bric Figlia sector of the CCZ), a low-to medium-angle, NNE-dipping, extensional sheared
20
693 Verrucano horizon, tens of meters long and up to few meters thick, suggest that the reactivation of
22
694 ENE- to NE-striking faults controlled the deposition of Lower Jurassic syn-extensional sediments
24
695 into elongated transtensional pull-apart basins ([Fig. 7B](#)).
26
28
30
32
337 The occurrence of different clastic to brecciated deposits at the base of the syn-extensional
34
35
36
37
38
39
400 deposition onto different terms of the pre-Jurassic succession (i.e., from the Variscan metamorphic
41
42
43
44
45
46
47
48
49
50
51
52
53
54
55
56
57
58
59
60
61
62
63
64
65

709 If we consider that a large amount of extensional displacement and crustal thinning is documented
 1
 710 to occurred during pre-Jurassic trastensional wrenching, our data suggest that extension along
 3
 711 low-angle detachment faults was not the only and most efficient mechanism in stretching and
 5
 712 thinning the CZ continental crust. This is also suggested by the lack of any Jurassic-related low-
 7
 713 angle extensional faults (i.e., corrugated surfaces) and associated cataclastic to mylonitic
 8
 714 deformation within the metamorphic basement and volcanic rocks, as commonly expected and
 12
 715 observed in both continental (e.g., [Sholz, 1987](#); [Bernoulli et al., 1990](#); [Manatschal, 2004](#); [Shipton et](#)
 14
 716 [al., 2006](#); [Handy et al., 2007](#); [Froitzheim et al., 2008](#)) and oceanic (e.g., [John, 1987](#); [Cann et al.,](#)
 16
 717 [1997](#); [Cannat, 1993](#); [Balestro et al., 2015, 2018](#); [Festa et al., 2015a](#); [Frassi et al., 2017](#)) settings,
 18
 718 independently on the time of deformation. On the contrary, a lithospheric wrenching controlled by a
 21
 719 new step of strike-slip faulting associated to an oblique rifting under a roughly E-W regional-scale
 23
 720 extension, which reactivates pre-existing Paleozoic faults and rheological weakness and
 25
 721 discontinuities, seems to better agree with the documented tectono-stratigraphic setting here
 27
 722 redefined for the CZ. As in the Southern Alps, the pre-Jurassic (i.e., Variscan to Permian – Early
 30
 723 Triassic) extension is, in fact, required to obtain the observed crustal extension, thinning and
 32
 724 mantle exhumation (see, e.g., [Handy et al., 1999](#); [Spalla et al., 2014](#); [Marotta et al., 2018](#) and
 34
 725 reference therein). Limited vertical displacement of syn-extensional Jurassic faults, clearly shows
 36
 726 that the contribute of emergent Jurassic faults and local low-to medium angle detachment ones,
 37
 727 was ineffective in producing and justifying the important crustal thinning inferred for the CZ
 39
 728 evolution as distal passive margin of Adria.

41
 42
 43
 44
 45
 46
 47
 48
 49
 50
 51
 52
 53
 54
 55
 56
 57
 58
 59
 60
 61
 62
 63
 64
 65

Although out of the aim of this work, we suggest that inferred detachment faults able to stretch the CZ continental crust, up to mantle exhumation, could be concentrated at deeper structural levels, which are not exposed in the studied sector. In continental crust, they are commonly expected to be characterized by significant deformation, ranging from gouge, cataclasites, and mylonities (e.g., [Caine et al., 1996](#); [Florineth and Froitzheim, 1994](#)) in several tens of meters-thick horizons (e.g., [Handy et al., 2007](#); [John and Cheadle, 2010](#); [Whitney et al., 2012](#)). On the contrary, if those detachment faults cut serpentinitized mantle rocks, they may evolve differently, as serpentinite can

737 create weaker faults, longer duration activity, and relatively low thickening gradient of fault zones
 1
 738 (e.g., [Nur Shuba et al., 2018](#) and reference therein). Although in the SCZ, potential primary
 3
 739 relationships between the serpentinitized peridotite and both Lower Permian volcanic rocks and
 5
 740 Middle-Upper Jurassic post-extensional sediments are not excluded to existed documenting
 7
 741 mantle exhumation, the occurrence of remnants of emergent detachment fault cutting serpentinite
 8
 742 is now masked and/or overprinted by Alpine tectonics.
 10
 11
 12
 13
 14

15 **6.3. Significance of the Canavese Zone in the geodynamic evolution of the Alpine** 16 **Tethys and Western Alps** 17 18

19
 2046 The documented different pulses of Late Carboniferous – Early Triassic strike-slip tectonics, which
 21
 2247 wrenched the already deformed Variscan metamorphic basement and controlled the Paleozoic
 23
 2448 deposition, is consistent with the long-lasting regional-scale wrench tectonics ([Fig. 8A](#); i.e., the
 25
 2649 “East-Variscan Shear Zone” *Auct.*), associated with the transition from Pangea B to Pangea A
 27
 2850 (*sensu* [Muttoni et al., 2003](#)) and the opening of the western Neo-Tethys during Early- to Late
 30
 3151 Permian time ([Fig. 8A](#)). This global-scale event, which reactivated the Variscan orogenic trends
 32
 3352 (e.g., [Matte, 1986](#); [Massari, 1988](#)), is inferred to have connected deep mechanical instabilities in
 34
 3553 the mantle with low crustal magmatism, and with wrenching of the upper crust across periodically
 36
 3754 active tectonic pathways (e.g., [Handy et al., 1999](#); [Muttoni et al., 2003](#); [Spalla et al., 2014](#) and
 38
 39
 4055 reference therein). The evidence and characteristics of Early Permian to Early Triassic strike-slip
 41
 4256 tectonics documented for the CZ may thus correspond to one of these regional-scale active
 43
 4457 tectonic pathways, which characterized large part of the Variscan belt North of the Adria
 45
 4658 microcontinent ([Fig. 8A](#)). Transtensional left-lateral kinematics documented in the studied sector,
 47
 48
 4959 along the ENE- to NE-striking faults, on the basis of geological mapping data (see also [Robustelli](#)
 50
 5160 [et al., 2018](#) for additional paleomagnetic constraints), well agree with those described by [Handy et](#)
 52
 5361 [al. \(1999\)](#) to the NE for the Cossato – Mergozzo – Brissago Line, and interpreted as a conjugate
 54
 5562 fault of the East-Variscan Shear Zone *Auct.* Alternatively, it is not excluded and possible to
 56
 57
 5863 discriminate in the studied sector, that the documented right- and left-lateral kinematics were, on
 59
 6064 the contrary, related to the switch of regional shortening from NW-SE to NE-SW directions as in
 61
 62
 63
 64
 65

765 the Southern Mediterranean Region (e.g., [Houari and Hoepffner, 2003](#); [Simancas et al., 2009](#);
766 [Michard et al., 2010](#)).

767

768 The close relationships between the Permian heating event and emplacement of post-Variscan
769 intrusives in the CZ, as well as in the whole Southern Alpine Domain, document the product of the
770 connection between crustal wrenching, related to strike-slip tectonics, and magmatic activity, which
771 in turn produced thermal perturbations leading to partial melting. During Early Permian, in fact, the
772 Adriatic lower crust was intruded by gabbros from the Northern Apennines (e.g., [Montanini and](#)
773 [Tribuzio, 2001](#)) to the Austroalpine (e.g., [Bussy et al., 2001](#); [Ballèvre et al., 2018](#)), and Southern
774 Alpine (e.g., [Pin, 1986](#); [Mayer et al., 2000](#)) domains, facilitated by deep-reaching transtentional
775 faults (e.g., [Rottura et al., 1998](#); [Handy et al., 1999](#)). Similar evolution developed in connection with
776 an “hot” strike-slip tectonics and volcanism, also occurred in Central Europe (e.g., [Muttoni et al.,](#)
777 [2003](#) and reference therein).

778

779 As it is largely documented that the onset of the Permian lithospheric wrenching, which drove the
780 Permian Pangea transformation, was favored by the Variscan orogenic inheritance (e.g.,
781 weakened state of the crust, reactivation of Variscan sutures, etc., see, e.g., [von Raumer et al.,](#)
782 [2013](#); [Spalla et al., 2014](#); [Marotta et al., 2018](#) for a complete review), our findings document that
783 the onset of the continental break-up and Jurassic rifting of the Alpine Tethys was strongly
784 controlled by Paleozoic structural inheritances also in the CZ ([Fig. 8](#)). Similar pre-existing high-
785 strain zones or suture zones were, in fact, documented controlling continental break-up and rifting
786 stages in different continental margins throughout the world (see, e.g., [Frimmel and Hartnady,](#)
787 [1992](#); [Basei et al., 2008](#); [Buitter and Torsvisk, 2014](#); [Petersen and Shiffer, 2016](#); [Will and Frimmel,](#)
788 [2018](#) for a complete review).

789

790 Alternative studies document that hyper-extension with crustal allochthonous separated by
791 exhumed mantle, often observed in magma-poor margins, can be explained by extension of
792 continental crust with pre-rift serpentinite preserved below (e.g., fossil mantle wedge; see [Peterson](#)
793
794
795

793 and Shiffer, 2016). Marotta et al. (2018) document, in fact, that if the Adria rifting developed in a
1
794 stable lithosphere, Triassic – Jurassic HT-LP metamorphism is predicted together with gabbro-
3
795 basalt production younger than 185 Ma instead of the observed Permian – Early Triassic
5
796 metamorphic and igneous record. Indeed, this has never been detected in the Alpine continental
7
797 crust, thus mantle serpentinization occurred before crustal-break up and the denudation occurred
9
10
1798 before ocean spreading (Marotta et al., 2018), and the opening of the Alpine Tethys did not start in
12
1799 a stable continental lithosphere but developed by recycling part of the old Variscan collisional
14
15
800 suture (Figs. 8B and 8C).
16

17
801
18
19
802 The occurrence of serpentinized peridotite in the SCZ is also strongly complicated by Alpine
21
803 tectonics (see Fig. 6). In fact, although mantle exhumation occurred in the Jurassic in the Alpine
23
804 Tethys, the primary architecture and size of the original ocean-continent transition zone (OCT)
25
805 from the Adria passive margin to the exhumed “continental mantle” (*sensu* Dilek and Furnes, 2011)
27
806 cannot be simply restored in the CZ because of Alpine-related deformation. It is important to note,
29
30
807 in fact, that the association of mantle and continental crustal rocks in the Rocca Canavese
32
33
808 Complex of the Sesia Zone (Figs. 2A and 9), which is tectonically juxtaposed to the SCZ through
34
809 the External Canavese Line, has been recently interpreted as the product of an Alpine-related
36
37
810 tectonic *mélange* (Roda et al., 2018). Similarly, the northeastern continuation of the CZ in the Biella
38
39
811 sector has been defined “Canavese tectonic *mélange*” by Berger et al. (2012), emphasizing once
41
42
812 again the significant mixing role of the Alpine tectonics.
43
44
813

45
46
814 Although out of the aim of this work, since Late Cretaceous the Alpine reactivation and inversion of
47
48
815 the long-lived Late Carboniferous to Jurassic inherited faults occurred, up to the present day
50
51
816 structural setting with the CZ sliced between the Sesia Zone and the Ivrea - Verbano Zone along
52
53
817 the External and Internal Canavese Lines, respectively. Therefore, our findings suggest that the
54
55
818 ENE- to NE-trending of part of the faults of the CZ, roughly represent an ancient (since Late
56
57
819 Carboniferous - Early Permian) and polyphasic major discontinuity and/or shear zone (i.e, the
59
820 Proto-Canavese Shear Zone), which controlled the evolution of the continental margin of Adria
61
62
63
64
65

821 from the onset of the East-Variscan Shear Zone (Figs. 8A) to the Jurassic rifting (Figs. 8B-D) and
 1
 822 subsequent Alpine collisional stages and exhumation (Fig. 9). Since the onset of the Jurassic
 3
 823 rifting, the Proto-Canavese Shear Zone likely controlled the segmentation of the continental margin
 5
 824 of Adria (compare Figs. 8B and 8C), separating the present day Sesia Zone from the Southern
 8
 825 Alps (Fig. 8D) through the formation of a narrow and elongated basin, gradually widening toward
 10
 826 SW (present-day coordinates), along which mantle spread out in forming the present day Lanzo
 12
 827 Ultramafic Complex (Piccardo, 2010) as a branch of the Alpine Tethys.

15
 828
 17
 829 During the collisional Alpine stage, the Canavese Shear Zone likely acted as a backstop of the
 18
 19
 830 accretionary complex (Fig. 9), separating the E- to SE-dipping Alpine subduction zone from the
 21
 831 Southern Alpine retrowedge. At this stage, it roughly corresponded to the Proto-Insubric Line
 23
 832 whose pre-collisional activity is also documented, according to our findings, to the NE in the Orobic
 25
 833 Southern Alps (see Zanchetta et al., 2015).

26
 834
 28
 835
 30
 836

7. Concluding remarks

32
 837
 34
 838

37
 838 Detailed geological mapping (1:5,000 scale) and stratigraphic and structural analyses, allowed to
 39
 839 define a new tectono-stratigraphic setting of the Variscan metamorphic basement and Paleozoic-
 41
 840 Cenozoic stratigraphic succession, and the tectonic evolution from the late Variscan stage to
 43
 841 Alpine ones in the framework of the continental break up of Pangea and exhumation of the Alpine
 45
 842 Tethyan mantle. Particularly, our finding document that the CZ corresponds to a narrow inherited,
 47
 843 and long-lived polyphasic strike-slip deformation zone (i.e., the Proto-Canavese shear zone), which
 50
 844 played a significant role in controlling the multistage tectonic evolution of this sector of the present-
 52
 845 day Western Alps from the late Variscan stage to the Alpine convergent stages and following
 54
 846 exhumation, passing through the Pangea continental break-up and the following Jurassic
 56
 847 exhumation of the Alpine Tethyan mantle. Thus, it is significant to outline that in the CZ the
 59
 848 Jurassic tectonic dismemberment of the distal passive margin of Adria, up to mantle rocks

61
 62
 63
 64
 65

849 exhumation, did not simply result from syn-rift Jurassic extension but was strongly favored by an
1
850 older structural inheritance (the Proto-Canavese Shear Zone), which controlled earlier lithospheric
3
851 weakness, as also suggested for other sectors of the Southern Alpine domain (e.g., [Cadel et al.,](#)
5
852 [1996; Spalla et al., 2014; Marotta et al., 2018](#)) for which the CZ represents the southwestern
7
853 prolongation. Our finding document a close affinity between: (i) the LMU and UMU of the Variscan
9
854 basement of the CZ and the Scisti dei Laghi polymetamorphic Complex and the Strona Ceneri
11
855 monometamorphic Complex of the Southern Alpine Domain (*Serie dei Laghi Auct.*), respectively,
13
856 and (ii) the Upper Carboniferous to Lower Cretaceous succession of the Lombardian Basin in the
15
857 Southern Alps.
17
18

19
20
21
22
23
24
25
26
27
28
29
30
31
32
33
34
35
36
37
38
39
40
41
42
43
44
45
46
47
48
49
50
51
52
53
54
55
56
57
58
59
60
61
62
63
64
65

In conclusion, our results demonstrate that in orogenic belts, characterized by structural and metamorphic complexities and polyphasic deformation as in the Western Alps, the recognizing and understanding of the role played by pre-Jurassic structural inheritances represent key factors that are essential for reconstructing not only the tectonic history from the continental break up of Pangea to the onset of the Alpine Tethyan oceanic basin, but the whole tectonic evolution of the orogenic belt. The large amount of extensional displacement and crustal thinning occurred during different pulses of Late Carboniferous – Early Triassic strike-slip tectonics is well-consistent with the role played by long-lived regional-scale wrench faults (e.g., the East-Variscan Shear Zone). This should be strongly taken in consideration in models aimed to understand processes and mechanisms of progressive stretching and lithospheric thinning, driving to the sharp decrease in crustal thickness and strong decoupling between upper crust and continental mantle, up to continental breakup and mantle exhumation of the Jurassic Alpine Tethys (i.e., the Ligurian – Piedmont Ocean). Thus, in complex orogenic belts, it is essential, and cannot be renounced to constrain multidisciplinary analytical studies (e.g. structural, stratigraphic, petrological) on new detailed geological maps (see also [Şengör, 2014](#)), and on the description of crosscutting relationships between stratigraphic uncoformities and mapped faults, if we aim to really understand their tectonometamorphic evolution, and better constrain palaeogeographic reconstructions.

877

1

878 **Acknowledgements**

879

880 This work was supported by research grants from Università di Torino (Ricerca Locale “ex 60%”
 881 2014–2017 to A. Festa) and from “Comune di Tavagnasco” to S. De Caroli and A. Succo. We
 882 extend our sincere thanks to Editor E. Saccani for inviting this contribution to Geoscience Frontiers.
 883 We thank E. Barbero, A. Centelli, P. Quagliolo, C. Robustelli, E. Zanella for insightful discussions
 884 on various aspects of the evolution of the Canavese Zone which were most helpful for the
 885 formulation of our ideas and interpretations presented in the paper. We are indebted and very
 886 grateful to S. Cavagna for who kindly and accurately prepared samples for petrological analyses.
 887

13

888 **References**

15

16

889

890

891

892

893

894

895

896

897

898

899

900

901

902

903

904

905

906

907

908

909

910

911

912

913

914

915

916

917

918

919

920

921

922

923

924

925

926

927

928

929

62

63

64

65

Ahrendt, H., 1972. Zur Stratigraphie, Petrographie und zum tektonischen Aufbau der Canavese – Zone und ihrer Lage zur Insubrischen Linie zwischen Biella und Courgnè (Norditalien). *Gottinger Arb. Geol. Palaont.*, 11, 1-89.

Argand, E., 1909. Sur la racine de la nappe rhétique. *Mitt. Schweiz. Geol. Komm.* 1, 1 – 7.

Armitage, J.J., Collier, J.S., Minshull, T.A., 2010. The importance of rift history for volcanic margin formation. *Nature* 465 (7300), 913–917.

Autin, J., Bellahsen, N., Leroy, S., Husson, L., Beslier, M-O., d’Acremont, E., 2013. The role of structural inheritance in oblique rifting: insights from analogue models and application to the Gulf of Aden. *Tectonophysics* 607, 51-64.

Baggio, P., 1963a. Osservazioni geologiche sulla Zona del Canavese nel tratto Courgnè – Issiglio (Prealpi Piemontesi). *Atti dell’Accademia di Scienze di Torino* 97, 1 – 22.

Baggio, P., 1963b. Sulla presenza di una serie Titonico –Cretacea nel Canavese s.s. (Prealpi Piemontesi). *Atti dell’Istituto Veneto di Scienze, Lettere ed Arti* 121, 215 – 234.

Baggio, P., 1965a. Caratteri stratigrafici e strutturali del Canavese s.s. nella zona di Montalto Dora. *Memorie dell’Istituto di Geologia Mineralogia Università di Padova* 25, 1 – 25.

Baggio, P., 1965b. Geologia della Zona del Canavese nel settore Levone – Courgnè (Prealpi Piemontesi). *Memoria dell’Accademia Patavina di Scienze, Lettere e Arti* 77, 41 – 71.

Balestro, G., Cadoppi, P., Perrone, G., Tallone, S., 2009. Tectonic evolution along the Col del Lis-Trana Deformation Zone (internal Western Alps). *Italian Journal of Geosciences* 128 (2), 331-339.

Balestro, G., Festa, A., Borghi, A., Castelli, D., Gattiglio, M., 2018. Role of Late Jurassic intra-oceanic structural inheritance in the Alpine tectonic evolution of the Monviso meta-ophiolite Complex (Western Alps). *Geological Magazine* 155 (2), 233-249.

Balestro, G., Festa, A., Dilek, Y., Tartarotti, P. 2015. Pre-Alpine extensional tectonics of a peridotite-localized oceanic core complex in the late Jurassic, high-pressure Monviso ophiolite (Western Alps). *Episodes* 38 (4), 266–82.

Ballèvre, M., Manzotti, P., Dal Piaz, G. V., 2018. Pre-Alpine (Variscan) inheritance: A key for the location of the future Valais Basin (Western Alps). *Tectonics* 37, 786-817.

- 930 Barnes, J.D., Beltrando, M., Lee Cin-Ty A., Cisneros, M., Loewy, S., Chin E., 2014. Geochemistry
931 of Alpine serpentinites from rifting to subduction: a view across paleogeographic domains
932 and metamorphic grade. *Chemical Geology* 389, 29-47.
- 933
934 Basei, M.A.S., Frimmel, H.E., Nutman, A.P., Preciozzi, F., 2008. West Gondwana amalgamation
935 based on detrital zircon ages from Neoproterozoic Ribeira and Dom Feliciano belts of
936 South America and comparison with coeval sequences from SW Africa. In: Pankhurst,
937 R.J., Trouw, R.A.J., De Brito Neves, B.B., de Wit, M.J. (Eds.), *West Gondwana: Pre-
938 Cenozoic Correlations Across the South Atlantic Region*. Geological Society of London
939 Special Publication 294, 239–256.
- 940
941 Bellahsen, N., Fournier, M., d’Acremont, E., Leory, S., Daniel, M.J, 2006. Fault reactivation and rift
942 localization: Northeastern Gulf of Aden margin. *Tectonics* 25 (1). TC1007. doi:
943 10.1029/2004TC001626
- 944
945 Beltrando, M., Compagnoni, R., Ferrando, S., Mohn, G., Frasca, G., Odasso, N., Vukmanovic, Z.,
946 2014. Crustal thinning and mantle exhumation in the Levone area (Southern Canavese
947 Zone, Western Alps). In: Manatschal, G., Mohn, G., Masini, E., and Beltrando, M. (Eds.),
948 *A Field Guide Across the Margins of Alpine Tethys*, Journal of the Virtual Explorer,
949 Electronic Edition 48, 6.
- 950
951 Beltrando, M., Frasca, G., Compagnoni, R., Vitale Brovarone, A., 2012. The Valaisan controversy
952 revisited: multi-stage folding of Mesozoic hyper-extended margin in the Petit St. Bernard
953 Pass area. *Tectonophysics* 579, 17-36.
- 954
955 Berger, A., Mercolli, I., Kapferer, N., 2012. Single and double exhumation of fault blocks in the
956 Internal Sesia – Lanzo Zone and the Ivrea – Verbano Zone (Biella, Italy). *International
957 Journal of Earth Sciences* 101 (7), 1877 – 1894.
- 958
959 Bernoulli, D., Bertotti, G., Froitzheim, N., 1990. Mesozoic faults and associated sediments in the
960 Austroalpine-South Alpine passive continental margin. *Memorie della Società Geologica
961 Italiana* 45, 25-38.
- 962
963 Berra, F., Galli, M.T.M, Reghellin, F., Torricelli, S., Fantoni, R., 2009. Stratigraphic evolution of the
964 Triassic – Jurassic succession in the Western Southern Alps (Italy): the record of the two
965 – stage rifting of the distal passive margin of Adria. *Basin Research* 21, 335 – 353.
- 966
967 Berra, F., Felletti, F., Tessarollo, A., 2016. Stratigraphic architecture of a transtensional continental
968 basin in low-latitude semiarid conditions: the Permian succession of the Central Orobic
969 Basin (Southern Alps, Italy). *Journal of Sedimentary Research* 86, 408-429.
- 970
971 Bertotti, G., 1991. Early Mesozoic extension and Alpine shortening in the western Souther Alps:
972 the geology of the area between Lugano and Menaggio (Lombardy, Northern Italy).
973 *Memorie di Scienze Geologiche, Padova* 43, 17-123.
- 974
975 Bertotti, G., Picotti, V., Bernoulli, D., Castellarin, A., 1993. From rifting to drifting: tectonic evolution
976 of the South- Alpine upper crust from the Triassic to the Early Cretaceous. *Sedimentary
977 Geology* 86, 53 – 76.
- 978
979 Biino, G., Castelli, D., Rossetti, P., 1986. Plutonisme acide et basique dans le socle de la Zone du
980 Canavese: relations entre le “granite de Belmonte” et les gabbros dans la region de
981 Cuorné (Alpes Occidentales). *C.R. Acad. Sc. Paris*. 16, 1473-1476.
- 982
983 Biino, G., Compagnoni, R., 1989. The Canavese Zone between the Serra d’Ivrea and the Dora
984 Baltea river (Western Alps). *Eclogae Geol. Helv.*, Bale 82, 413 – 417.
- 985

- 986 Bonini, M., Souriot, T., Boccaletti, M., Brun, J.-P., 1997. Successive orthogonal and oblique
 987 extension episodes in a rift zone: laboratory experiments with application to the Ethiopian
 988 Rift. *Tectonics* 16 (2), 347–362.
- 989
 990 Borghi, A., Compagnoni, R., Naldi, M., 1996. The crystalline basement of the Canavese Zone
 991 (Internal Western Alps): new data from the area west of Ivrea. *Géol. Alpine* 72, 23 – 34.
- 992
 993 Boriani, A., Origoni Giobbi, E., 2004. Does the basement of the western southern Alps display a
 994 tilted section through the continental crust? A review and discussion. *Per. Minerl.* 73, 5-22.
- 995
 996 Boriani, A., Giobbi Origoni, E., Borghi, A., Caironi, V., 1990. The evolution of the “Serie dei Laghi”
 997 (Strona-Ceneri and Scisti dei Laghi): the upper component of the Ivrea-Verbanò crustal
 998 section; Southern Alps, North Italy and Ticino, Switzerland. *Tectonophysics* 182, 103-118.
- 999
 1000 Boriani, A., Sacchi, R., 1974. The “Insubric” and other tectonic lines in the Southern Alps (NE Italy).
 1001 *Memorie della Società Geologica Italiana* 13, 1-11.
- 1002
 1003 Brun, J.P., Beslier, M.O., 1996. Mantle exhumation at passive margins. *Earth Planetary Science*
 1004 *Letters* 142, 161-173.
- 1005
 1006 Brune, S., Popov, A.A., Sobolev, S.V., 2012. Modeling suggests that oblique extension facilitates
 1007 rifting and continental break-up. *Journal of Geophysical Research* 117 (B8), B08402.
- 1008
 1009 Buiter, S.J.H., Torsvik, T.H., 2014. A review of Wilson Cycle plate margins: a role for mantle plumes
 1010 in continental break-up along sutures? *Gondwana Research* 26, 627–653.
- 1011
 1012 Bussy, F., von Raumer, J., Capuzzo, N., 2001. Mont Blanc-Aiguilles rouges Massifs (External
 1013 Massifs)—An example of polyorogenic evolution. *Mémoires de Géologie Lausanne* 36,
 1014 53–84.
- 1015
 1016 Cadel, G., Cosi, M., Pennacchioni, G., Spalla, M.I., 1996. A new map of the Permo-Carboniferous
 1017 cover and Variscan metamorphic basement in the central Orobic Alps, Southern Alps-
 1018 Italy: structural and stratigraphical data. *Memoria di Scienze Geologiche, Padova* 48, 1-
 1019 53.
- 1020
 1021 Caine, J.S., Evans, J.P., Forster, C.B., 1996. Fault zone architecture and permeability structure.
 1022 *Geology* 24, 1025–1028.
- 1023
 1024 Cann, J.R., Blackman, D.K., Smith, D.K., McAllister, E., Janssen, B., Mello, S., Avgerinos, E.,
 1025 Pascoe, A.R., Escartin, J., 1997. Corrugated slip surfaces formed at ridge-transform
 1026 intersections on the Mid-Atlantic Ridge. *Nature* 385, 329–332.
- 1027
 1028 Cannat, M., 1993. Emplacement of mantle rocks in the seafloor at Mid-Ocean ridge. *Journal of*
 1029 *Geophysical Research* 98(B3), 4163–72.
- 1030
 1031 Cassinis, G., Perotti, C.R., Ronchi, A., 2012. Permian continental basins in the Southern Alps (Italy)
 1032 and peri-Mediterranean correlations. *International Journal of Earth Sciences* 101, 129-
 1033 157.
- 1034
 1035 Clerc, C., Lagabrielle, Y., 2014. Thermal control on the modes of crustal thinning leading to mantle
 1036 exhumation: insights from the Cretaceous Pyrenean hot paleomargins. *Tectonics* 33 (7),
 1037 1340-1359.
- 1038
 1039 Clerc, C., Lagabrielle, Y., Neumaier, M., Reynaud, J.Y., de Saint Blanquat, M., 2012. Exhumation
 1040 of subcontinental mantle rocks: evidence from ultramafic-bearing clastic deposits nearby
 1041 the Lherz peridotite body, French Pyrenees. *Bull. la Soc. G_eol. Fr.* 183 (5), 443e459.

- 1042
1043 Clerc, C., Ringenbach, J-C., Jolivet, L., Ballard, J-F, 2018. Rifted margins: ductile deformation,
1044 boudinage, continentward-dipping normal faults and the role of the weak lower crust.
1045 Gondwana Research 53, 20-40.
1046
- 1047 Cochran, J.R., Karner, G.D., 2007. Constraints on the deformation and rupturing of continental
1048 lithosphere of the Red Sea: the transition from rifting to drifting. In: Karner, G.D.,
1049 Manatschal, G., Pinheiro, L.M. (Eds.), *Imaging, Mapping and Modelling Continental
1050 Lithosphere Extension and Breakup*. Geological Society Special Publications 282, 265-
1051 289.
1052
- 1053 Contrucci, I., Matias, L., Moulin, M., Geli, L., Klingelhofer, F., Nouze, H., Aslanian, D., Olivet, J.L.,
1054 Rehault, J.P., Sibuet, J.C., 2004. Deep structure of the West African continental margin
1055 (Congo, Zaire, Angola), between 5_S and 8_S, from reflection/refraction seismics and
1056 gravity data. *Geophys. J. Int.* 158, 529-553.
1057
- 1058 Dal Piaz, G.V., Bistacchi, A., Massironi, M., 2003. Geological outline of the Alps. *Episodes* 26, 175-
1059 180.
1060
- 1061 Dilek, Y., Furnes, H., 2011. Ophiolite genesis and global tectonics: geochemical and tectonic
1062 fingerprinting of ancient oceanic lithosphere. *Geological Society of America Bulletin* 123
1063 (2/3), 387-411.
1064
- 1065 Direen, N.G., Stagg, H.M.J., Symonds, P.A., Colwell, J.B., 2008. Architecture of volcanic rifted
1066 margins: new insights from the Exmouth–Gascoyne margin, Western Australia. *Australian
1067 Journal of Earth Sciences* 55, 341–363.
1068
- 1069 Dunbar, J.A., Sawyer, D.S., 1989. How preexisting weaknesses control the style of continental
1070 breakup. *Journal of Geophysical Research* 94 (B6), 7278–7292.
1071
- 1072 Elter, G., Elter, P., Sturani, C., Weidmann, M., 1966. Sur la prolongation du domaine ligure de
1073 l'Appennin dans le Monferrat et les Alpes et sur l'origine de la Nappe de la Simme s.l. des
1074 Préalpes rondes et chablaisiennes. *Arch. Sci. Genève* 19, 279 – 377.
1075
- 1076 Fazlikhani, H., Fossen, H., Gawthorpe, R.L., Faleide, J.I., Bell, R.E., 2017. Basement structure and
1077 its influence on the structural configuration of the northern North Sea rift. *Tectonics*, 36,
1078 1151–1177.
1079
- 1080 Fenoglio, M., 1956. La massa peridotitico-serpentinosa di Castellamonte e il suo significato
1081 geologico. *Estr. Rend. Soc. Min. It.* 12, pp 10.
1082
- 1083 Festa, A., Balestro, G., Dilek, Y., Tartarotti, P., 2015a. A Jurassic oceanic core complex in the
1084 high-pressure Monviso ophiolite (western Alps, NW Italy). *Lithosphere* 7, 646–52.
1085
- 1086 Festa, A., Dilek, Y., Codegone, G., Cavagna, S., Pini, G.A., 2013. Structural anatomy of the
1087 Ligurian accretionary wedge (Monferrato, NW Italy), and evolution of superposed
1088 mélanges. *Geological Society of America Bulletin* 125 (9–10), 1580–1598.
1089
- 1090 Festa, A., Ogata, K., Pini, G.A., Dilek, Y., Codegone, G., 2015b. Late Oligocene–early Miocene
1091 olistostromes (sedimentary mélanges) as tectono-stratigraphic constraints to the
1092 geodynamic evolution of the exhumed Ligurian accretionary complex (Northern
1093 Apennines, NW Italy). *International Geology Review* 57 (5–8), 540–562.
1094
- 1095 Ferrando, S., Bernoulli, D., Compagnoni, R., 2004. The Canavese Zone (Internal Western Alps): a
1096 distal margin of Adria. *Schweiz. Mineral. Petrog. Mitt.* 84, 237 – 256.
1097

- 1098 Florineth, D., Froitzheim, N., 1994. Transition from continental to oceanic basement in the Tasna
1099 nappe (Engadine window, Graubünden, Switzerland): evidence for Early Cretaceous
1100 opening of the Valais ocean. *Schweizer Mineralogische und Petrographische Mitteilungen*
1101 74, 437–478.
- 1102
1103 Franchi, S., Mattiolo, S., Novarese, V., Stella, A., 1912. Geological Map of Italy at 1:100,000
1104 scale, Sheet 42 “Ivrea”. I ed., Regio Ufficio Geologico d’Italia, Roma.
- 1105
1106 Frasca, G., Gueydan, F., Brun, J-P-, Monié, P., 2016. Deformation mechanisms in a continental rift
1107 up to mantle exhumation. Field evidence from the western Betics, Spain. *Marine and*
1108 *Petroleum Geology* 76, 310-328.
- 1109
1110 Frassi, C., Musumeci, G., Zucali, M., Mazzarini, F., Rebay, G., Langone, A., 2017. The Cotoncello
1111 Shear Zone (Elba Island, Italy): the deep root of a fossil oceanic detachment fault in the
1112 Ligurian ophiolites. *Lithos* 278-281, 445-463.
- 1113
1114 Frimmel, H.E., Hartnady, C.J.H., 1992. Blue amphiboles and their significance for the metamorphic
1115 history of the Pan-African Gariep belt, Namibia. *Journal of Metamorphic Geology* 10, 651–
1116 669.
- 1117
1118 Froitzheim, N., Derks, J.F., Walter, J.M., Sciunnach, D., 2008. Evolution of an Early Permian
1119 extensional detachment fault from synintrusive, mylonitic flow to brittle faulting (Grassi
1120 Detachment Fault, Orobic Anticline, southern Alps, Italy). *Geological Society of London*
1121 *Special Publication* 298, 69–82.
- 1122
1123 Froitzheim, N., Eberli, G.P., 1990, Extensional detachment faulting in the evolution of a Tethys
1124 passive continental margin, eastern Alps, Switzerland: *Geological Society of America*
1125 *Bulletin* 102, 1297–1308.
- 1126
1127 Garde, A.A., Boriani, A., Sørensen, E.V., 2015. Crustal modelling of the Ivrea-Verbano zone in
1128 northern Italy re-examined: coseismic cataclasis versus extensional shear zones and
1129 sideways rotation. *Tectonophysics* 662, 291-311.
- 1130
1131 Giobbi Mancini, E., Boriani, A., Villa, I., 2003. Pre Alpine ophiolites in the basement of Southern
1132 Alps: the presence of a bimodal association (LAG – Leptyno-Amphibolitic Group) in the
1133 Serie dei Laghi (N-Italy, Ticino-CH). *Rend. Fis. Acc. Lincei* 9 (14), 79-99.
- 1134
1135 Giobbi Origoni, E., Testa, B., Carimati, R., 1982. Contributo alla ricostruzione stratigrafica della
1136 “Serie dei Laghi”: litofacies principali della “Strona-Ceneri” a NE del Lago Maggiore (Alpi
1137 Meridionali – Italia). *Rendiconti della Società Italiana di Mineralogia e Petrologia* 38 (3),
1138 1337-1350.
- 1139
1140 Giuntoli, F., Engi, M., 2016. Internal geometry of the central Sesia Zone (Aosta Valley, Italy): HP
1141 tectonic assembly of continental slices. *Swiss Journal of Geosciences* 109 (3), 445-471.
- 1142
1143 Handy, M., Franz, L., Heller, F., Janott, B., Zurbruggen, R., 1999. Multistage accretion and
1144 exhumation of the continental crust (Ivrea crustal section, Italy and Switzerland).
1145 *Tectonics* 18, 1154–1177.
- 1146
1147 Handy, M.R., Hirth, G., Bürgmann, R., 2007. Continental fault structure and rheology from the
1148 frictional-to-viscous transition downward. In: *Tectonic Faults: Agents of Change on a*
1149 *Dynamic Earth*, Cambridge, MA, pp. 139–181.
- 1150
1151 Handy, M.R., Steit, J.E., 1999. Mechanics and mechanisms of magmatic underplating: inferences
1152 from mafic veins in deep crustal mylonite. *Earth and Planetary Science Letters* 16, 271-
1153 286.

62

63

64

65

- 1154
1155 Handy, M. R., Zingg, A., 1991. The tectonic and rheological evolution of an attenuated cross
1156 section of the continental crust: Ivrea crustal section, southern Alps, northwestern Italy
1157 and southern Switzerland. *Geological Society of America Bulletin* 103(2), 236–53.
1158
- 1159 Houari, M.R., Hoepffner, C., 2003. Late Carboniferous dextral wrench-dominated transpression
1160 along the North African craton margin (Eastern High Atlas, Morocco). *Journal of African*
1161 *Earth Sciences* 37, 11–24.
1162
- 1163 John, B.E., 1987. Geometry and evolution of a mid-crustal extension fault sys-tem: Chemehuevi
1164 Mountains, southeastern California. *Geological Society of London Special Paper* 28, 313–
1165 335.
1166
- 1167 John, B.E., Cheadle, M.J., 2010. Deformation and alteration associated with oceanic and
1168 continental detachment fault systems: are they similar? In: Rona, P.A., De-vey, C.W.,
1169 Dymont, J., Murton, B.J. (Eds.), *Diversity of Hydrothermal Systems on Slow Spreading*
1170 *Ocean Ridges*. In: *Geophysical Monograph Series*, Washington D.C., vol. 188, pp. 175–
1171 205.
1172
- 1173 Lanza, R., 1984. Paleomagnetism in the Traversella massif. *Boll. Geof. Teor. Appl.* 26, 115 –124.
1174
- 1175 Lundin, E.R., Doré, A.G., 2011. Hyperextension, serpentization, and weakening: a new paradigm
1176 for rifted margin compressional deformation. *Geology* 39, 347–350.
1177
- 1178 Manatschal, G., 2004. New models for evolution of magma-poor rifted margins based on a
1179 review of data and concepts from West Iberia and the Alps. *Int. J. Earth Sci.* 93, 432-466.
1180
- 1181 Manatschal, G., Froitzheim, N., Rubenach, M., Turrin, B., 2001. The role of detachment faulting in
1182 the formation of an ocean-continent transition: insights from the Iberia abyssal plain. *Geol.*
1183 *Soc. Lond. Spec. Publ.* 187 (1), 405-428.
1184
- 1185 Manatschal, G., Lavier, L., Chenin, P., 2015. The role of inheritance in structuring hyperextended rift
1186 systems: some considerations based on observations and numerical modeling. *Gondw.*
1187 *Res.* 27, 140-164.
1188
- 1189 Manzotti, P., Ballèvre, M., Zucali, M., Robyr, M., Engi, M., 2014. The tectonometamorphic evolution
1190 of the Sesia–Dent Blanche nappes (internal Western Alps): Review and synthesis. *Swiss*
1191 *Journal of Geosciences* 107, 309–336.
1192
- 1193 Marotta, A.M., Roda, M., Conte, K., Spalla, M.I., 2018. Thermo-mechanical numerical model of the
1194 transition from continental rifting to oceanic spreading: the case study of the Alpine
1195 Tethys. *Geological Magazine* 155 (2), 250-279.
1196
- 1197 Masini, E., Manatschal, G., Mohn, G., Unternehr, P., 2012. Anatomy and tectono-sedimentary
1198 evolution of a rift-related detachment system: the example of the Err detachment (central
1199 Alps, SE Switzerland). *Geological Society of America Bulletin* 124 (9/10), 1535-1551.
1200
- 1201 Massari, F., 1988. Some thoughts on the Permo-Triassic evolution of the South-Alpine area (Italy).
1202 In: Cassinis, G. (ed.), *Permian and Permian-Triassic boundary in the South-Alpine*
1203 *segment of the Western Tethys, and additional regional reports*. *Memorie della Società*
1204 *Geologica d'Italia* 34, 179-188.
1205
- 1206 Matte, P., 1986. Tectonics and plate tectonics model for the Variscan belt of Europe.
1207 *Tectonophysics* 126 (2-4), 329-335, 347-332,344-374.
1208

- 1209 Michard, A., Soulaïmani, A., Hoepffner, C., Ouanaimi, H., Daidder, L., Rjijmati, E.C., Saddqi, O.,
1210 2010. The South-western branch of the Variscan Belt: evidence from Morocco.
1211 Tectonophysics 492, 1-24.
1212
- 1213 Mohn, G., Manatschal, G., Müntener, O., Beltrando, M., Masini, E., 2010. Unravelling the
1214 interaction between tectonic and sedimentary processes during lithospheric thinning in the
1215 Alpine Tethys margins. *Int. J. Earth Sci.* 99, 75-101.
1216
- 1217 Montanini, A., Tribuzio, R., 2001. Gabbro-derived granulites from the Northern Apennines (Italy):
1218 Evidence for lower-crustal emplacement of tholeiitic liquids in post-Variscan times. *Journal*
1219 *of Petrology* 42, 2259-2277.
1220
- 1221 Moulin, M., Aslanian, D., Olivet, J.L., Klingelhoefer, F., Nouz_e, H., Rehault, J.P., Unterneuhr, P.,
1222 2005. Geological constraints on the evolution of the Angolan margin based on reflection
1223 and refraction seismic data (Zaiango Project). *Geophys. J. Int.* 162, 793-810.
1224
- 1225 Mulch, A., Rosenau, M., Dorr, W., Handy, M.R., 2002. The age and structure of dikes along the
1226 tectonic contact of the Ivrea-Verbano and Strona-Ceneri Zones (southern Alps, Northern
1227 Italy, Switzerland). *Schwizerische Mineralogische und Petrographische Mitteilungen* 82,
1228 55-76.
1229
- 1230 Muttoni, G., Kent, D.V., Garzanti, E., Brack, P., Abrahamsen, N., Gaetani, M., 2003. Early Permian
1231 Pangea 'B' to Late Permian Pangea 'A'. *Earth and Planetary Science Letters* 215 (3), 379-
1232 394.
1233
- 1234 Novarese, V., 1929. La Zona del Canavese e le formazioni adiacenti. *Mem. Descr. Carta Geol. It.*
1235 22, 65 – 212.
1236
- 1237 Nur Shuba, C., Gray, G.G., Morgan, J.K., Sawyer, D.S., Shillington, D.J., Reston, T.J., Bull, J.M.,
1238 Jordan B.E., 2018. A low-angle detachment fault revealed: three-dimensional images of
1239 the S-reflector fault zone along the Galicia passive margin. *Earth and Planetary Science*
1240 *Letter* 492, 232-238.
1241
- 1242 Osmundsen, P.T., Ebbing, J., 2008. Styles of extension offshore mid-Norway and implications for
1243 mechanisms of crustal thinning at passive margins. *Tectonics* 27, TC6016.
1244
- 1245 Péron-Pinvidic, G., Manatschal, G., Minshull, T.A., Sawyer, D.S., 2007. Tectonosedimentary
1246 evolution of the deep Iberia-Newfoundland margins: evidence for a complex breakup
1247 history. *Tectonics* 26, 1-29.
1248
- 1249 Perrone, G., Eva, E., Solarino, S., Cadoppi, P., Balestro, G., Fioraso, G., Tallone S., 2010.
1250 Seismotectonic investigations in the inner Cottian Alps (Italian Western Alps): An
1251 integrated approach. *Tectonophysics* 496, 1-4.
1252
- 1253 Petersen, K.D., Schiffer, C., 2016. Wilson cycle passive margins: control of orogenic inheritance on
1254 continental breakup. *Gondwana Research* 39, 131–144.
1255
- 1256 Phillips, T.B., Jackson, C.A.-L., Bell, R.E., Duffy, O.B., Fossen, H., 2016. Reactivation of
1257 intrabasement structures during rifting: A case study from offshore southern Norway.
1258 *Journal of Structural Geology* 91, 54–73.
1259
- 1260 Piccardo, G., 2010. The Lanzo peridotite massif, Italian Western Alps: Jurassic rifting of the
1261 Ligurian Tethys. *Geological Society Special Publication* 337, 47-69.
1262

- 1263 Pin, C., 1986. Datation U–Pb sur zircon à 285 Ma du complexe gabbro dioritique du Val Sesia - Val
1264 Mastallone et age tardi hercynien du métamorphisme granulitique de la zone Ivrea-
1265 Verbano (Italie). *Compte Rendu Academie des Sciences de Paris* 303, 827–30.
- 1266
1267 Quick, J.E., Sinigoi, S., Peressini G., Demarchi, G., Wooden, J.L., Sbisà, A., 2009. Magmatic
1268 plumbing of a large Permian caldera exposed to a depth of 25 km. *Geol. Soc. Am.* 37(7),
1269 603 – 606.
- 1270
1271 Quick, J.E., Sinigoi, S., Snoke, A.W., Kalakay, T.J., Mayer, A., Peressini, G., 2003. Geological Map
1272 of the Southern Ivrea-Verbanò Zone, Northwestern Italy. USGS – Geologic Investigations
1273 Series Map I-2776, 22 pp.
- 1274
1275 Ranero, C., Perez-Gussinyé, M., 2010. Sequential faulting explains the asymmetry and extension
1276 discrepancy of conjugate margins. *Nature* 468 (7321), 294-299.
- 1277
1278 Robustelli, C., Balestro, G., Centelli, A., De Caroli, S., Succo, A., Zanella, E., Festa, A., 2018.
1279 Paleomagnetic and magnetic fabric constraints for the structural evolution of polyphasic
1280 strike-slip shear zones: the example of the Canavese Zone (Western Alps, Italy).
1281 *Geophysical Research Abstracts* 20, EGU2018-1799. EGU General Assembly 2018.
- 1282
1283 Roda, M., De Salvo, F., Zucali, M., Spalla, M.I., 2018. Structural and metamorphic evolution during
1284 tectonic mixing: is the Rocca Canavese Thrust Sheet (Italian Western Alps) a subduction-
1285 related mélangé? *Italian Journal of Geosciences* 137, 311-329.
- 1286
1287 Ronchi, A., Santi, G., 2003, Non-marine biota from the Lower Permian of the Central Southern
1288 Alps (Orobic and Collio Basins, N Italy): a key to the paleoenvironment. *Geobios* 36, 749-
1289 760.
- 1290
1291 Rottura, A., Bargossi, G.M., Caggianelli, A., Del Moro, A., Visonà, D., Tranne, C.A., 1998. Origin
1292 and signi-
1293 Southern Alps, Italy. *Lithos* 45. 329-348.
- 1294
1295 Sacchi, R., Quagliolo, P., Strona, A., 2007. Il settore sud-occidentale della Zona Strona-Ceneri nel
1296 Biellese e Canavese. *Boll. Mus. Sci. Nat. Torino* 24(1), 5-24.
- 1297
1298 Schettino, A., Turco, E., 2011. Tectonic history of the western Tethys since Late Triassic.
1299 *Geological Society of America Bulletin* 123 (1/2), 89-105.
- 1300
1301 Schmid, S.M., Fugenschuh, B., Kissling, E., Schuster, R., 2004. Tectonic map and overall
1302 architecture of the Alpine orogen. *Eclogae Geol. Helv.* 97, 93-110.
- 1303
1304 Schmid, S.M., Zingg, A., Handy, M., 1987, The kinematics of movements along the Insubric Line
1305 and the emplacement of the Ivrea Zone. *Tectonophysics* 135, 47-66.
- 1306
1307 Scholz, C.H., 1987. Wear and gouge formation in brittle faulting. *Geology* 15, 493–495.
- 1308
1309 Shipton, Z.K., Soden, A.M., Kirkpatrick, J.D., Bright, A.M., Lunn, R.J., 2006. How thick is a fault?
1310 Fault displacement-thickness scaling revisited. In: Abercrombie, R., McGarr, A., DiToro,
1311 G., Kanamori, H. (Eds.), *Earthquakes: Radiated Energy and the Physics of Faulting*, 193–
1312 198.
- 1313
1314 Schuster, R., Stüwe, K., 2008. Permian metamorphic event in the Alps. *Geology* 36, 603–6.
- 1315
1316 Şengör, A.M.C., 2014. How scientometry is killing science. *GSA Today* 24 (12), 44-45.
- 1317
1318 Simancas, J.F., Azor, A., Martínez Poyatos, D.J., Tahiri, A., El, Hadi H., González-Lodeiro, F.,
1319 Pérez-Estaún, A., Carbonell, R., 2009. Tectonic relationships of Southwest Iberia with the

- 1319 allochthons of Northwest Iberia and the Moroccan Variscides. *Comptes Rendus*
 1320 *Geoscience* 341, 103–113.
- 1321
- 1322 Smye, A.J., Stockli, D.F., 2014. Rutile U-Pb age depth profiling: A continuous record of lithospheric
 1323 thermal evolution. *Earth and Planetary Science Letters* 408, 171–82.
- 1324
- 1325 Spalla, M.I., Lardeaux, J.M., Dal Piaz, G.V., Gosso, G., 1991. Metamorphisme et tectonique a la
 1326 marge externe de la zone Sesia-Lanzo (Alpes occidentales). *Memorie di Scienze*
 1327 *Geologiche* 43, 361–9.
- 1328
- 1329 Spalla, M. I., Zanoni, D., Marotta, A. M., Rebay, G., Roda, M., Zucali, M. & Gosso, G. 2014. The
 1330 transition from Variscan collision to continental break-up in the Alps: insights from the
 1331 comparison between natural data and numerical model predictions. In *The Variscan*
 1332 *Orogeny: Extent, Timescale and the Formation of the European Crust* (eds K. Schulmann,
 1333 J. R. Martínez Catalán, J. M. Lardeaux, V. Janoušek & G. Oggiano), pp. 363–400.
 1334 Geological Society, London, Special Publication no. 405.
- 1335
- 1336 Stampfli, G.M., Borel, G.D., Marchant, R., Mosar, J., 2002. Western Alps geological constraints of
 1337 western Tethyan reconstructions. In: Rosemaum, G. and Lister, G.S. (Eds.),
 1338 *Reconstruction of the evolution of the Alpine-Himalayan Orogen*. *Journal of Virtual*
 1339 *Explorer* 7, 75-104.
- 1340
- 1341 Sturani, C., 1964. Prima segnalazione di Ammoniti del Lias del Canavese. *Rendiconti*
 1342 *dell'Accademia dei Lincei*, Roma 37, 1-6.
- 1343
- 1344 Sturani, C., 1973. Considerazioni sui rapporti tra Appennino settentrionale ed Alpi occidentali.
 1345 *Rendiconti dell'Accademia dei Lincei*, Roma 183, 119-142.
- 1346
- 1347 Talwani, M., Eldholm, O., 1972. Continental margin off Norway: a geophysical study. *Geological*
 1348 *Society of America Bulletin* 83 (12), 3575–3606.
- 1349
- 1350 von Raumer, J. F., Bussy, F., Schaltegger, U., Schulz, B., Stampfli, G. M. 2013. Pre-Mesozoic
 1351 Alpine basements: Their place in the European Paleozoic framework. *Geological Society*
 1352 *of America Bulletin* 125(1–2), 89–108.
- 1353
- 1354 Zanchetta, S., Malusà, M.G., Zanchi, A., 2015. Precollisional development and Cenozoic evolution
 1355 of the Southalpine retrobelt (European Alps). *Lithosphere* 7 (6), 662-681.
- 1356
- 1357 Zingg, A., Handy, M.R., Hunziker, J.C., Schmid, S.M., 1990. Tectonometamorphic history of the
 1358 Ivrea Zone and its relationship to the crustal evolution of the Southern Alps.
 1359 *Tectonophysics* 182(1), 169-192.
- 1360
- 1361 Zingg, A., Hunziker, J.C., Frey, M., Ahrendt, H., 1976. Age and degree of metamorphism of the
 1362 Canavese Zone and of the sedimentary cover of the Sesia Zone. *Schweiz. Mineral.*
 1363 *Petrogr. Mitt.*, 56, 361-365.
- 1364
- 1365 Whitney, D.L., Teyssier, C., Rey, P., Buck, W.R., 2012. Continental and oceanic core complexes.
 1366 *Geological Society of America Bulletin* 125, 273–298.
- 1367
- 1368 Will, T.M., Frimmel, H.E., 2018. Where does continent prefer to break up? Some lessons from the
 1369 South Atlantic margins. *Gondwana Research* 53, 9-19.
- 1370
- 1371 Wolfenden, E., Ebinger, C., Yirgu, G., Deino, A., Ayalew, D., 2004. Evolution of the northern Main
 1372 Ethiopian rift: birth of a triple junction. *Earth and Planetary Science Letters* 224 (1–2),
 1373 213–228.
- 1374

1375 Wozniak J., 1977. Contribution à l'étude géologique des Alpes Occidentales Internes: la region du
1376 Canavese. Ph.D Thesis, Univ. Pierre et Marie Curie, Paris, 146 pp.
1377
1378

4
5
6
7
8
9
10
11
12
13
14
15
16
17
18
19
20
21
22
23
24
25
26
27
28
29
30
31
32
33
34
35
36
37
38
39
40
41
42
43
44
45
46
47
48
49
50
51
52
53
54
55
56
57
58
59
60
61
62
63
64
65

Figure captions

Figure 1 – (A) Structural sketch of the Alps-Apennine orogenic system (modified from Festa et al., 2015b) and location of the map shown in Figure 1B. (B) Tectonic map of the Northwestern Alps and the Northern Apennines (modified from Balestro et al., 2015) with the location of the studied sector (red line).

Figure 2 – (A) Structural sketch of the Canavese Zone (CZ), displaying the tectonic relationships with the Ivrea-Verbanò Zone and Sesia Zone, and related stratigraphic columnar sections (not to scale), showing the tectono-stratigraphic relationships between the different lithological units in the Southern (SCZ), Central (CCZ) and Northern (NCZ) sectors of the CZ (thickness of the lithostratigraphic units are in the text). *Mantle rocks*: Serpentinite (SRP); *Variscan basement*: Lower Metamorphic Unit (LMU), Amphibolite (AMP), Upper Metamorphic Unit (UMU); *Early to Middle Permian post-Variscan intrusives*: Gabbro and Diorite (GBD), Granite and Tonalite (GRT), Hypoabissal dykes (HBD), Leucogranite (LGR); *Upper Carboniferous to Middle Triassic pre-extensional succession*: Basal Conglomerate (CGB; Late Carboniferous - Early Permian); Volcanics (COL1), Volcanoclastics (COL1a) and lacustrine deposits (COL2) of the Collio Formation (Early Permian); Verrucano (VER, Late Permian); Dolostone (DOL, Middle Triassic); *Lower - Middle Jurassic syn-extensional succession*: Clastic member (MUF1), Arenaceous member (MUF2), Siltitic-Arenaceous member (MUF3), and Limestone member (MUF4) of the Muriaglio Formation (Early – Middle Jurassic); *Upper Jurassic - Lower Cretaceous post-extensional succession*: Shaly member (SEL1) and Siliceous member (SEL2) of the Selcifero Lombardo (Middle - Late Jurassic); Calpionella Limestone (CAL, Tithonian - Berriasian); Palombini Limestone (APA, Early Cretaceous). (B) Representative mesoscale data (Schmidt net, lower hemisphere) of main Alpine-related strike-slip faults bounding and crosscutting the CZ succession: (1) transpressional left-lateral faults, and (2) superposed transtensional right-lateral ones; (n.: number of fault planes; black arrows represent slickenslines; blue, green and red squares show the maximum, intermediate and minimum shortening axes, respectively).

Figure 3 – Images of the Variscan metamorphic units and Paleozoic lithostratigraphic units and structures at different scales: **(A)** Close-up photo of the tectonic contact (dashed red line) between Serpentinite (SRP) and the Selcifero Lombardo (SEL1) to the NW of Mt. Piedmonte in the SCZ; **(B)** Close-up of the intrusive relationships (blue line) between diorite (GBD) and the migmatitized orthogneiss of the Lower Metamorphic Unit (LMU) in the CCZ (T. Piova area), both injected (black lines) by the leucogranite (LGR). Note that the set of fractures, which is parallel to the fault (dashed red line) is filled by leucogranite injection. Dashed black lines indicate the Variscan foliation; **(C)** Close-up view of the intrusive contact (dashed white lines) of the granophyre hypoabissal dyke (HBD) with the orthogneiss of the Lower Metamorphic Unit (LMU), close to Vidracco village in the CCZ. Dashed black lines indicate the Variscan foliation. Hammer for scale; **(D)** Close-up of the amphibolite characterizing the mafic horizon, which separates the LMU and UMU of the Variscan metamorphic basement in the CCZ (SSE of Bric Figlia); **(E)** Well-bedded (dashed white line) alternating medium-grained metasandstone and fine-grained metasilstone of the Upper Metamorphic Unit in the CCZ (South of Bric Figlia), deformed by Late-Variscan open folds. Hammer for scale; **(F)** Close-up view of the diorite (GBD) intruded (dashed white line) by a granite dyke (GRT) in the NCZ (ESE of Borgofranco d’Ivrea); **(G)** Close-up photograph of the continental fluvial deposits of the Basal Conglomerate (Late Carboniferous), showing rounded to irregular clasts, consisting of fragments of quartz veins, metasandstone, micascist, and gneiss, embedded in coarse-grained arenite of the same composition of clasts (CCZ, close to Serra Alta); **(H)** Close-up view of the angular unconformity (dotted blue line) superposing the Verrucano (VER; Late Permian) onto both the metasediments of the UMU and the Volcanic Member of the Collio Formation (COL1, Late Permian) to the South of Bric Figlia in the CCZ (dashed white line represents the attitude of bedding). The yellow dotted line represents the unconformity at the base of the Collio Formation. Hammer for scale; **(I)** Polished sample of the sheared Verrucano horizon, showing the strong elongation of clasts according to a roughly ENE-oriented extensional stretching direction (ENE of Bric Figlia in the CCZ).

Figure 4 – Simplified geological map (**A**) of the Central Canavese Zone (Bric Figlia area) and related geological cross-sections (**B** and **C**), showing the tectono-stratigraphic relationships between the different terms of the Variscan metamorphic basement and the overlying Paleozoic- to Mesozoic stratigraphic succession. Restored cross sections (**D** and **E**) at the Middle – Late Jurassic time show the tectonic control of pre-Jurassic inherited faults in the deposition of the Permian succession (Collio Formation and Verrucano), as documented by the abrupt change of thickness of these lithostratigraphic units in sectors bounded by faults (see text for details). The “null point” indicates the change from extension/transension to net contraction/transpression. Acronyms of the lithostratigraphic units as in Figure 2.

Figure 5 – Images of the Mesozoic lithostratigraphic units and structures at different scales: (**A**) Panoramic view of the stratigraphic contact (dotted blue line) between the Middle Triassic platform Dolostone (DOL) and the syn-extensional succession of the Muriaglio Formation (MUF) in Montalto Dora, NCZ; (**B-D**) Close-up view of different facies of the Clastic Member of the Muriaglio Formation through the CZ. In the CCZ (E of Bric Figlia) it shows (**B**) clast-to matrix-supported polymictic angular to sub-angular clasts (orthogneiss, amphibolite and metasandstone of the Variscan metamorphic basement, volcanic, granitoid, and rare dolostone fragments), embedded in a coarse-grained yellowish to reddish matrix (pencil for scale). In the SCZ (N of Levone) (**C**) it differs on a major content of Triassic dolomitic clasts, which are mostly lacking (**D**) in the NCZ (Montalto Dora); (**E**) Close-up of the Arenaceous Member of the Muriaglio Formation, showing medium- to coarse grained sandstone, passing upward to dark-reddish fine- to medium grained sandstone and siltstone (Muriaglio in the CCZ); (**F**) Close-up view of the Siltitic-arenaceous Member of the Muriaglio Formation, showing dark gray pelitic to fine-grained sandstone levels, alternating to grayish sandstone, in cm-thick horizons (Montalto Dora in the NCZ); (**G**) Close-up photograph of the Limestone Member of the Muriaglio Formation, consisting of alternating limestone and sandstone in decimeters thick beds (Montalto Dora in the NCZ); (**H**) Close-up view of the reddish argillite, alternating with yellowish-greenish pelite of the Selcifero Lombardo close to Muriaglio in the CCZ; (**I**) Outcrop view of alternating reddish to pinkish

1464 radiolarian-bearing cherts and shale (i.e., *Radiolarites Auct.*) of the Selcifero Lombardo (E of
 1465 Campo C.se in the CCZ); **(L)** Outcrop view of the Internal Canavese Line (ICL; red line) at
 1466 Montalto Dora in the NCZ, which tectonically juxtaposes the gabbro of the Ivrea-Verbano Zone
 1467 (IVZ) to the Limestone Member of the Muriaglio Formation of the Canavese Zone succession
 1468 (CZ). This mylonitic contact is displaced by brittle faults (black lines). Dashed white lines indicate
 1469 the mylonitic foliation; **(M)** Panoramic view of a transtensional flower structure (dashed red lines)
 1470 within the shear zone of the External Canavese Zone, which juxtaposes the Sesia Zone with the
 1471 Muriaglio Formation of the Canavese Zone (E of Borgofranco d'Ivrea in the NCZ); **(N)** Close-up
 1472 view of a transtensional strike-slip duplex developed in the uppermost part of the metasandstone
 1473 of the Upper Metamorphic Unit (UMU) of the Variscan basement (Bric Filia in the CCZ). This type
 1474 of structures commonly displace the overlying Collio Formation and Verrucano with the same
 1475 geometry. Hammer for scale.

Figure 6 – Simplified geological map **(A)** of the Southern Canavese Zone (Levone area) and
 related geological cross-sections **(B and C)**. Note that the primary position of Triassic dolostone,
 which is now totally lacking in outcrop because of the intense quarry activity, has been restored
 on the basis of literature data ([Novarese, 1929](#); [Baggio, 1965a](#)).

Figure 7 – **(A)** Schematic cross-section showing the tectono-stratigraphic relationships between
 pre-Middle Triassic inherited faults and sediment deposition in the CZ. Note the tectonic control
 of faults in the deposition of the Permian succession (Collio Formation and Verrucano).
 Acronyms of the lithostratigraphic units as in Figure 2. **(B)** Simplified sketch (map view, not to
 scale), showing the relationships between reactivated inherited strike-slip faults, ENE- to NE-
 striking (red lines), and newly formed extensional faults, NW-striking (black line), at the onset of
 the Early Jurassic extension. The interlacing between these high-angle faults, and possibly local
 low-angle detachment faults (dotted blue line), controlled the deposition of the Lower Jurassic
 syn-extensional sediments of the Muriaglio Formation into elongated transtensional pull-apart
 basins. Thick red arrows indicated the regional direction of extension.

1492
 1
 1493 **Figure 8** –Paleogeographic reconstructions (in map) of: **(A)** the Variscan Belt at Early Permian,
 3 showing its complex structural zonation related to wrench tectonics along main dextral strike-slip
 1494 fault zones (e.g., the East-Variscan Shear Zone) and associated left-lateral ones (modified from
 5
 1495 [Ballèvre et al., 2018](#), and from [Stampfli et al., 2002](#); [Schettino and Turco, 2011](#)); **(B)** the onset of
 8
 1496 the continental break-up at Late Triassic (modified from [Stampfli et al., 2002](#); [Schettino and](#)
 10
 1497 [Turco, 2011](#)), showing its close relation with the strike-slip faults inherited from the Early Permian
 12
 1498 wrench tectonics (dashed red lines); **(C)** the location of the active rifting of the future Alpine
 14
 1499 Tethys and continental crust thinning at Early Jurassic (modified from [Stampfli et al., 2002](#);
 16
 1500 [Schettino and Turco, 2011](#)). In all figures, the location of the Canavese Zone (blu star) is inferred
 18
 1501 from [Stampfli et al. \(2002\)](#) and [Schettino and Turco \(2011\)](#). **(D)** Schematic regional cross-section
 20
 1502 through the Alpine Tethys at Late Jurassic – Early Cretaceous (modified from [Manzotti et al.,](#)
 22
 1503 [2014](#)), showing the location of the “Proto-Canavese Shear Zone” at the distal passive margin of
 24
 1504 the Adria microplate.
 26
 28
 1505
 30
 1506

1507 **Figure 9** – **(A)** Paleogeographic reconstructions (in map) of the Alpine Tethyan realm in the Late
 34
 1508 Cretaceous (modified from [Stampfli et al., 2002](#); [Schettino and Turco, 2011](#); [Festa et al., 2013](#)),
 36
 1509 showing the location of the Canavese Zone, and its potential role as a backstop of the Alpine
 37
 1510 accretionary complex, separating the E- to SE-dipping Alpine subduction zone from the Southern
 39
 1511 Alpine retrowedge, during Late Cretaceous **(B)** and Late Eocene **(C)** convergent stages
 41
 1512 (modified from [Manzotti et al., 2014](#)). **(D)** Simplified cross-section, showing the Late Oligocene –
 43
 1513 Early Miocene right-lateral reactivation of the Canavese Shear Zone during the exhumation of
 45
 1514 the Sesia Zone (modified from [Manzotti et al., 2014](#)).
 47
 48
 1515
 50
 1516
 52
 53
 54
 55
 56
 57
 58
 59
 60
 61
 62
 63
 64
 65

Figure 1
[Click here to download high resolution image](#)

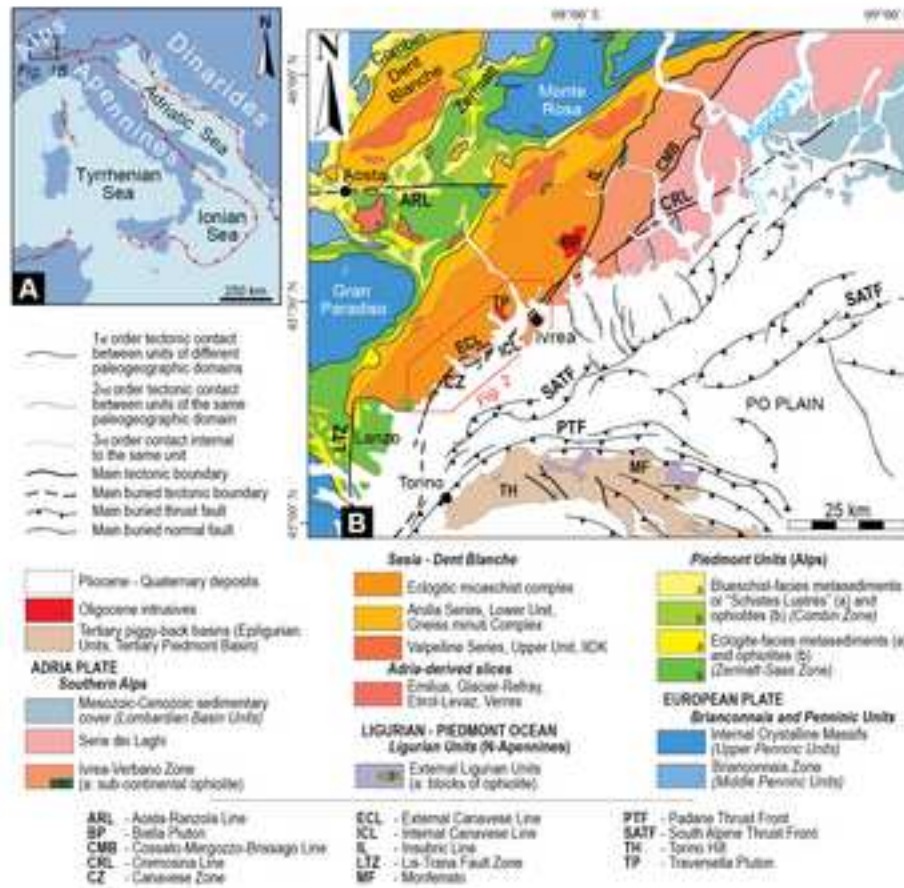


Figure 1 - Festa et al_Geoscience Frontiers (width 140 mm)

Figure 2
[Click here to download high resolution image](#)

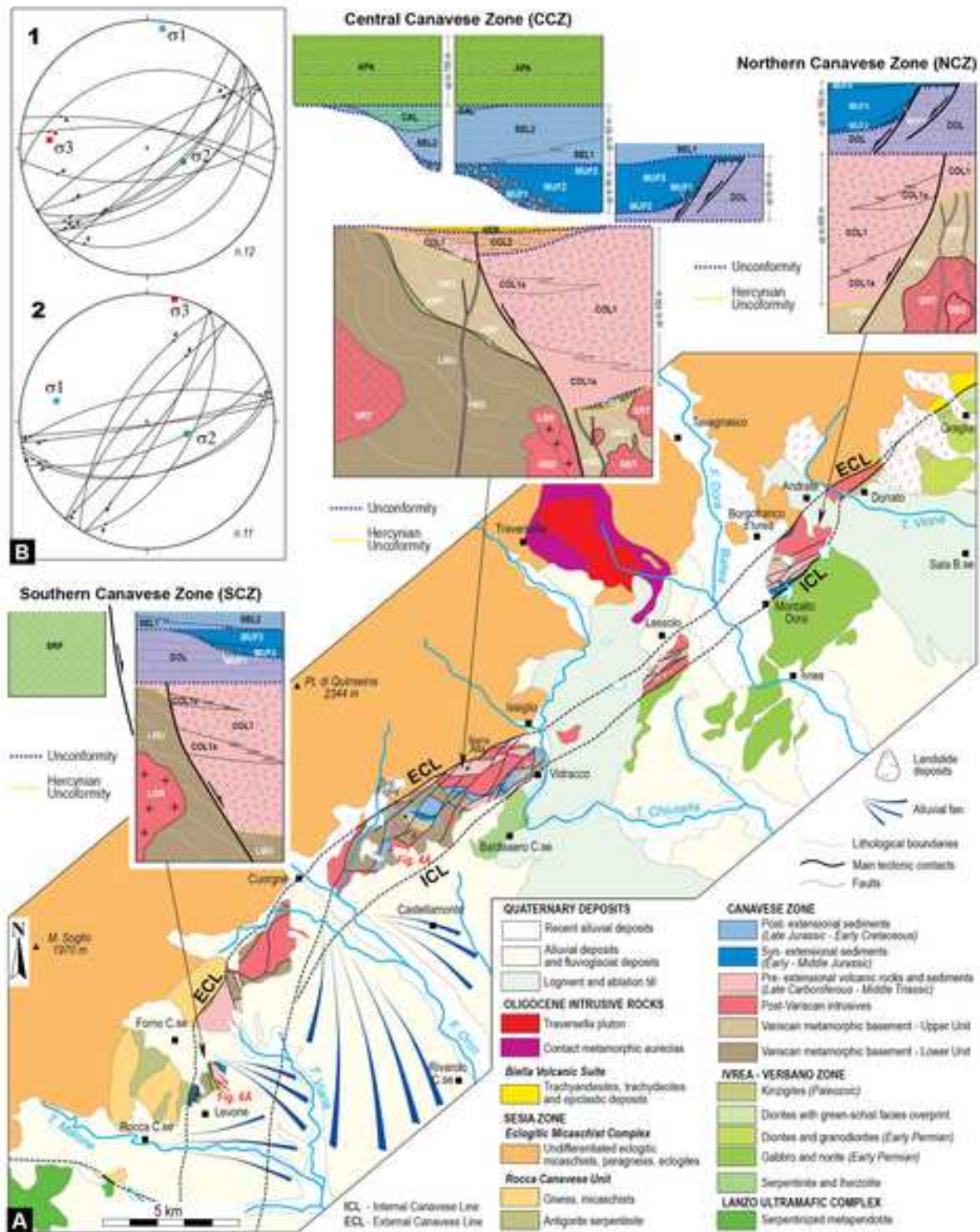


Figure 2 - Festa et al_Geoscience Frontiers (190 mm X 240 mm)

Figure 3
[Click here to download high resolution image](#)

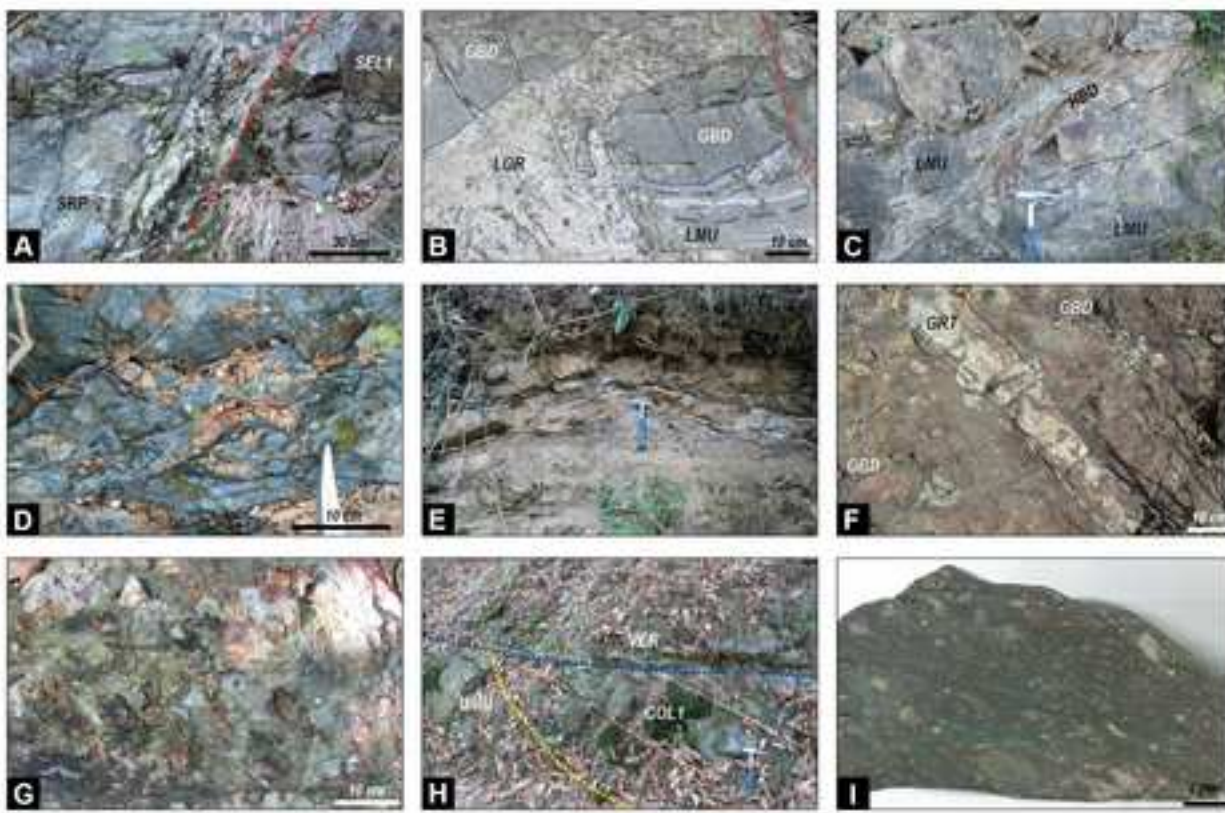


Figure 3 - Festa et al_ *Geoscience Frontiers* (width 190 mm)

Figure 4
[Click here to download high resolution image](#)

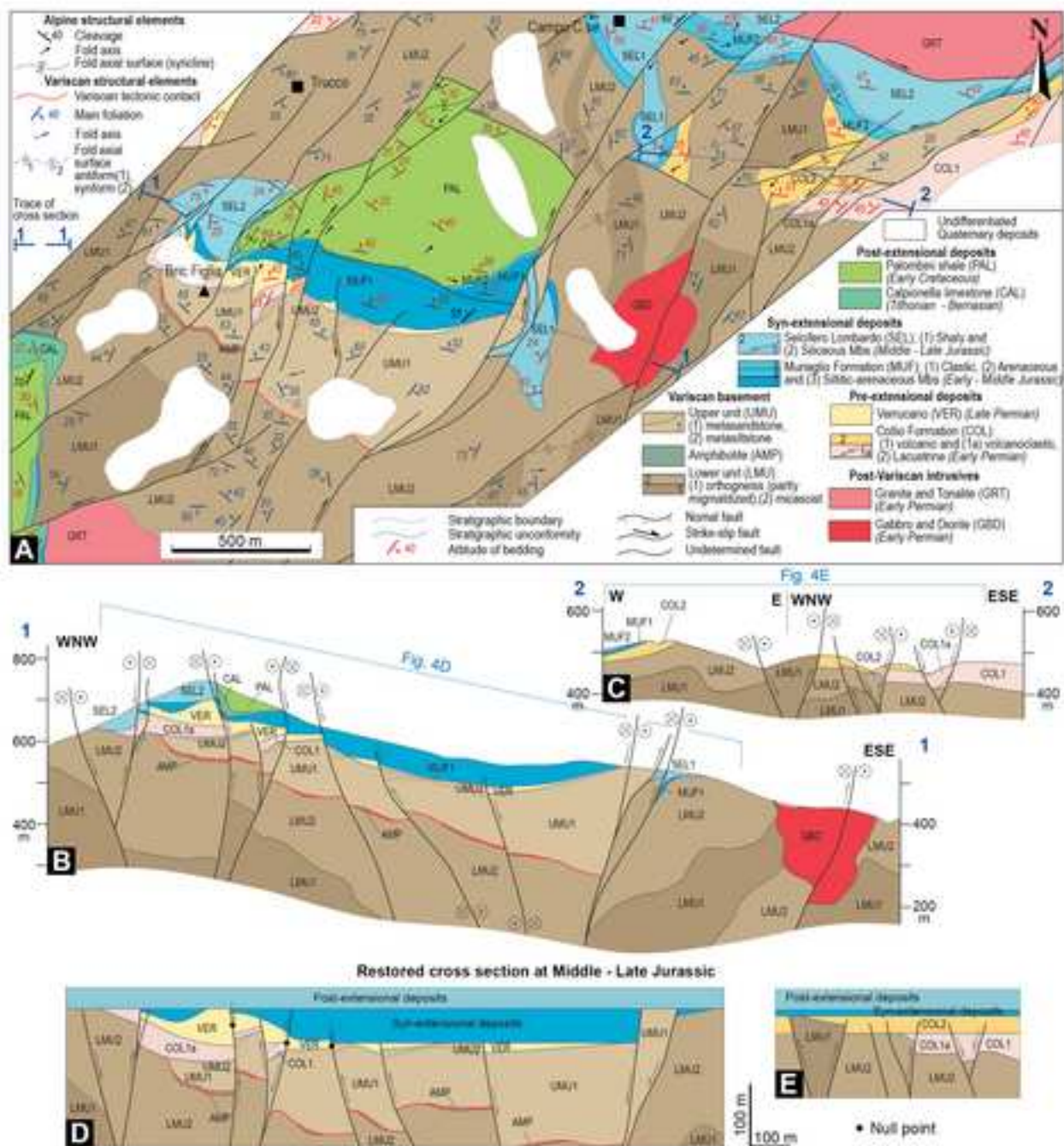


Figure 4 - Festa et al_ Geoscience Frontiers (width 190 mm)

Figure 5
[Click here to download high resolution image](#)

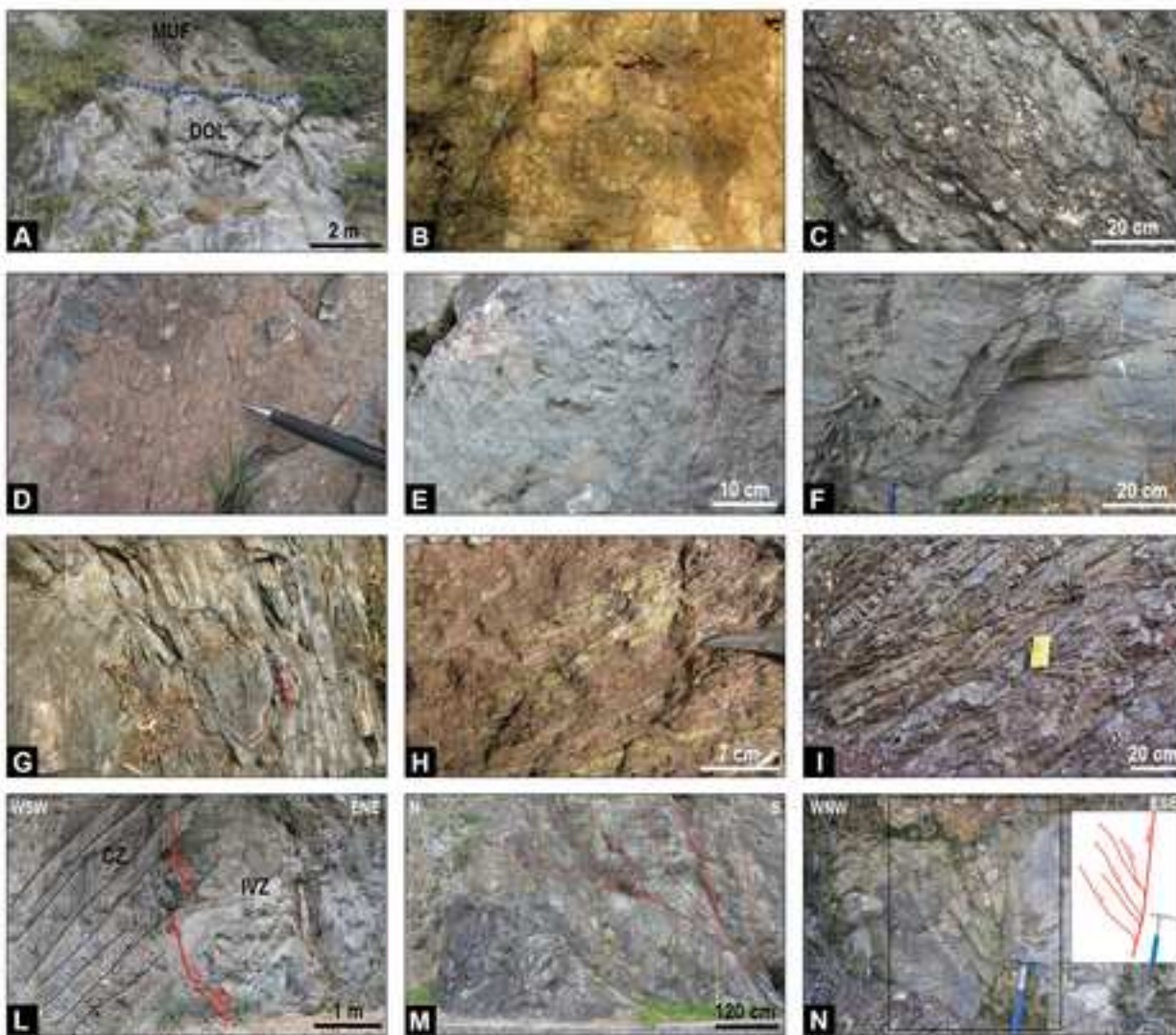


Figure 5 - Festa et al_ *Geoscience Frontiers* (width 190 mm)

Figure 6
[Click here to download high resolution image](#)

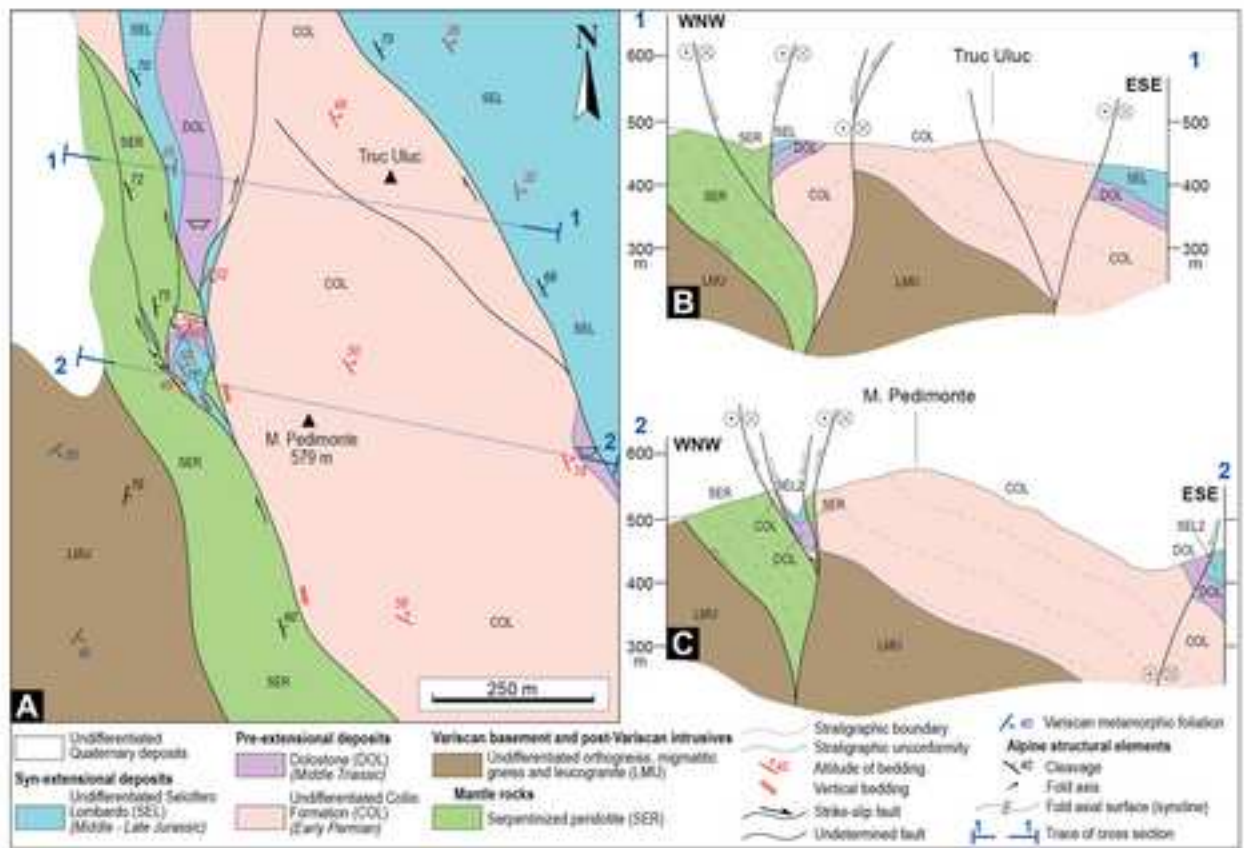


Figure 6 - Festa et al *Geoscience Frontiers* (width 190 mm)

Figure 7

[Click here to download high resolution image](#)

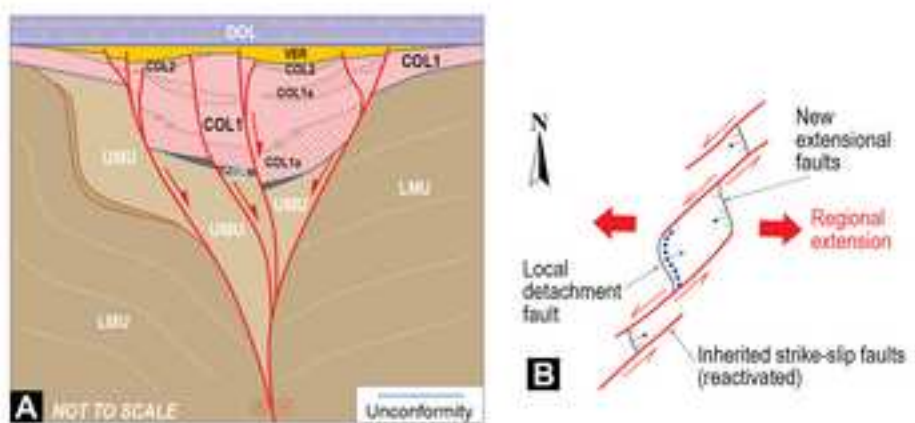


Figure 7 - Festa et al_ *Geoscience Frontiers* (width 140 mm)

Figure 8
[Click here to download high resolution image](#)

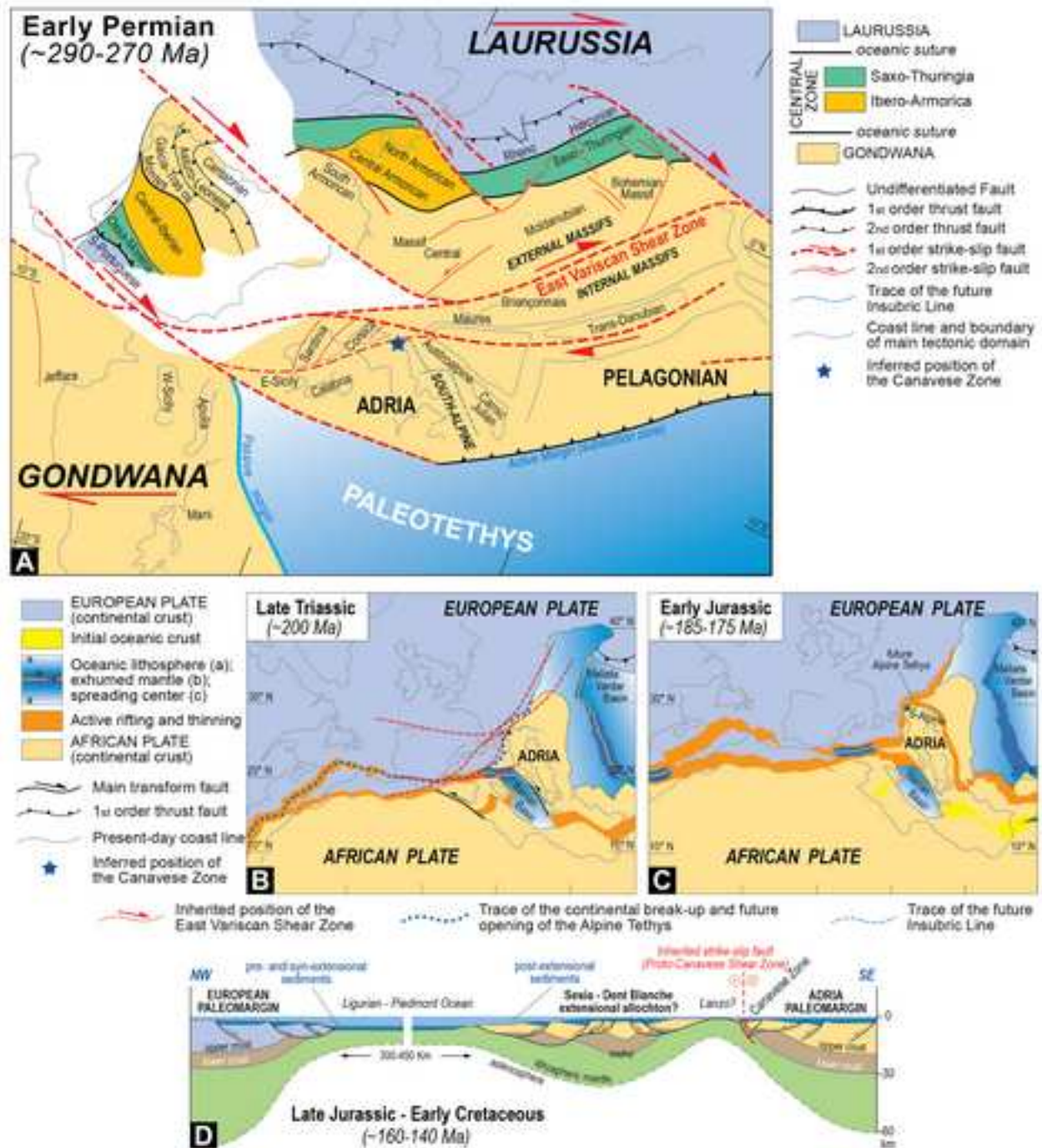


Figure 8 - Festa et al_Geoscience Frontiers (width 190 mm)

Figure 9

[Click here to download high resolution image](#)

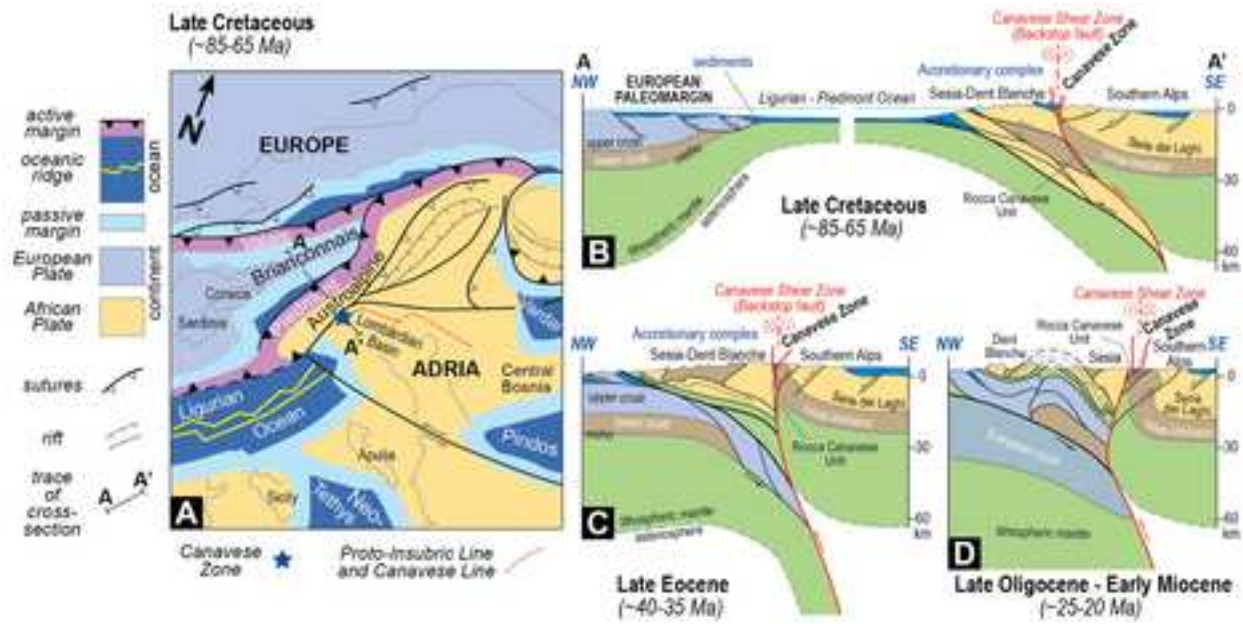


Figure 9 - Festa et al *Geoscience Frontiers* (width 190 mm)